

Hole-mediated ferromagnetism in tetrahedrally coordinated semiconductors

T. Dietl[†]

*Research Institute of Electrical Communication, Tohoku University, Katahira 2-1-1,
Sendai 980-8577, Japan and Institute of Physics and College of Science,
Polish Academy of Sciences, al. Lotników 32/46, PL-00-668 Warszawa, Poland*

H. Ohno and F. Matsukura

*Laboratory for Electronic Intelligent Systems, Research Institute of Electrical Communication,
Tohoku University, Katahira 2-1-1, Sendai 980-8577, Japan*

(Dated: October 25, 2018)

A mean field model of ferromagnetism mediated by delocalized or weakly localized holes in zinc-blende and wurzite diluted magnetic semiconductors is presented. The model takes into account: (i) strong spin-orbit and kp couplings in the valence band; (ii) the effect of strain upon the hole density-of-states, and (iii) the influence of disorder and carrier-carrier interactions, particularly near the metal-to-insulator transition. A quantitative comparison between experimental and theoretical results for (Ga,Mn)As demonstrates that theory describes the values of the Curie temperatures observed in the studied systems as well as explain the directions of the easy axis and the magnitudes of the corresponding anisotropy fields as a function of biaxial strain. Furthermore, the model reproduces unusual sign, magnitude, and temperature dependence of magnetic circular dichroism in the spectral region of the fundamental absorption edge. Chemical trends and various suggestions concerning design of novel ferromagnetic semiconductor systems are described.

I. INTRODUCTION

The discovery of ferromagnetism in zinc-blende^{1,2} III-V and^{3,4} II-VI Mn-based compounds allows one to explore physics of previously not available combinations of quantum structures and magnetism in semiconductors. For instance, a possibility of changing the magnetic phase by light in⁵ (In,Mn)As/(Al,Ga)Sb and³ (Cd,Mn)Te/(Cd,Zn,Mg)Te heterostructures was put into the evidence. The injection of spin-polarized carriers from (Ga,Mn)As to a (In,Ga)As quantum well in the absence of an external magnetic field was demonstrated, too.⁶ It is then important to understand the ferromagnetism in these semiconductors, and to ask whether the Curie temperatures T_C can be raised to above 300 K from the present 110 K observed for $\text{Ga}_{0.947}\text{Mn}_{0.053}\text{As}$.^{2,7}

In this paper, we develop theory of the hole-mediated ferromagnetism in tetrahedrally coordinated semiconductors along the lines of a model proposed recently by us.⁸ Since we aim at quantitative description of experimental findings, the proposed theoretical approach⁸ makes use of empirical facts and parameters wherever possible. We begin the present paper by discussing electronic states in p-type magnetic semiconductors. We classify the studied systems as charge transfer insulators, so that our theory is not applicable to materials in which d electrons participate in charge transport. We note that Mn ions act as both source of localized spins and effective mass acceptors. We adapt, therefore, the physics of the metal-insulator transition in doped semi-

conductors for the studied case, and assume that over the relevant range of impurity concentrations, the ferromagnetic exchange is mediated by delocalized or weakly localized holes. Since the resulting spin-spin coupling is long range, we use a mean field approximation to determine various thermodynamic, magnetoelastic, and optical properties of the system. Particular attention is paid to take carefully into account the complex structure of the valence band. We then present results of comprehensive numerical studies which provide qualitative, and in many cases quantitative, interpretation of experimental finding accumulated over the recent years for (Ga,Mn)As. This good agreement between experimental and theoretical data encourages us to show, in the final part of the paper, expected chemical trends, and to propose various suggestions concerning the design of novel ferromagnetic semiconductor systems.

In general terms, our results point to the importance of the kp and spin-orbit interactions in the physics of the hole-mediated ferromagnetism in semiconductors. These interactions control the magnitude of Curie temperature, saturation value of magnetization, and character of magnetic anisotropies. A comparison of theoretical and experimental findings not only emphasizes similarities and differences between III-V magnetic semiconductors and other ferromagnetic systems, but demonstrates also novel aspects of half metallic ferromagnets. The recent comprehensive reviews present many aspects of III-V,⁹ II-VI,¹⁰ as well as of IV-VI magnetic semiconductors,¹¹ which will not be discussed here.

II. ELECTRONIC STATES IN P-TYPE MAGNETIC SEMICONDUCTORS

A Mn ion in tetrahedrally coordinated semiconductors

We consider zinc-blende or wurzite semiconductor compounds, in which the cations are partly substituted by magnetic ions, such as Mn. The magnetic ions are assumed to be randomly distributed over the cation sites, as found by extended x-ray absorption fine structure (EXAFS) studies in the case of $\text{Ga}_{1-x}\text{Mn}_x\text{As}$ ¹² and $\text{Cd}_{1-x}\text{Mn}_x\text{Te}$.¹³ The Mn provides the localized spin $S = 5/2$ and, in the case of III-V semiconductors, acts as an acceptor. These Mn acceptors compensate the deep antisite donors commonly present in GaAs grown by low-temperature molecular beam epitaxy, and produce a p-type conduction with metallic resistance for the Mn concentration x in the range $0.04 \leq x \leq 0.06$.^{7,14,15,16} Accurate analysis of the transport data, complicated by a large magnitude of the extraordinary Hall effect, confirms the presence of a strong compensation,¹⁷ presumably by As antisite donors, as mentioned above. However, at this stage we cannot exclude the existence of self-compensation mechanisms, such as the formation of Mn AX-like centers or donor defects once the Fermi level reaches an appropriately deep position in the valence band.¹⁸

According to optical studies, Mn in GaAs forms an acceptor center characterized by a moderate binding energy¹⁹ $E_a = 110$ meV, and a small magnitude of the energy difference between the triplet and singlet state of the bound hole^{19,20} $\Delta\epsilon = 8 \pm 3$ meV. This small value demonstrates that the hole introduced by the divalent Mn in GaAs does not reside on the d shell or forms a Zhang-Rice-like singlet,^{21,22} but occupies an effective mass Bohr orbit.^{8,23} Thus, due to a large intra-site correlation energy U , (Ga,Mn)As can be classified as a charge-transfer insulator, a conclusion consistent with photoemission spectroscopy.^{24,25} At the same time, the p-d hybridization results in a spin-dependent coupling between the holes and the Mn ions, $H_{pd} = -\beta N_o \mathbf{sS}$. Here β is the p-d exchange integral and N_o is the concentration of the cation sites. The analysis of both photoemission data^{24,25} and magnitude²³ of $\Delta\epsilon$ leads to the exchange energy $\beta N_o \approx -1$ eV. Similar values of βN_o are observed in II-VI diluted magnetic semiconductors with comparable lattice constants.²⁶ This confirms Harrison's suggestion that the hybridization matrix elements depend primarily on the inter-atomic distance.²⁷ According to the model in question, the magnetic electrons remain localized at the magnetic ion, so that they do not contribute to charge transport. This precludes Zener's double exchange²⁸ as the mechanism leading to ferromagnetic correlation between the distant Mn spins. At the same time, for some combinations of transition metals and hosts, the "chemical" and exchange attractive potential introduced by the magnetic ion can be strong enough to bind the hole on

a local orbit.^{21,22} In an intermediate regime, the probability of finding the hole around the magnetic ion is enhanced, which results in the apparent increase of $|\beta N_o|$ with decreasing x .²²

B Two-fluid model of electronic states near the metal-insulator transition

Ionized impurity and magnetic scatterings lead to localization of the effective mass holes introduced by Mn in III-V compounds or by acceptors in the case of II-VI materials. It is, therefore, important to discuss the effect of Anderson-Mott localization on the onset of ferromagnetism. The two-fluid model²⁹ constitutes the established description of electronic states in the vicinity of the Anderson-Mott metal-insulator transition (MIT) in doped semiconductors. According to that model, the conversion of itinerant electrons into singly occupied impurity states with increasing disorder occurs gradually, and begins already on the metal side of the MIT. This leads to a disorder-driven static phase separation into two types of regions: one populated by electrons in extended states, and another that is totally depleted from the electrons or contains singly occupied impurity-like states. The latter controls the magnetic response of doped non-magnetic semiconductors²⁹ and gives rise to the presence of bound magnetic polarons (BMP) on both sides of the MIT in magnetic semiconductors.^{26,30,31} Actually, the formation of BMP shifts the MIT towards the higher carrier concentrations.^{26,30,31} On crossing the MIT, the extended states become localized. However, according to the scaling theory of the MIT, their localization radius ξ decreases rather gradually from infinity at the MIT towards the Bohr radius deep in the insulator phase, so that on a length scale smaller than ξ the wave function retains an extended character. Such weakly localized states are thought to determine the static longitudinal and Hall conductivities of doped semiconductors. The central suggestion of the recent model⁸ is that the holes in the extended or weakly localized states mediate the long-range interactions between the localized spins on both sides of the MIT in the III-V and II-VI magnetic semiconductors.

As will be discussed below, the Curie temperature T_C is proportional to the thermodynamic spin density-of-states ρ_s which, in turn, is proportional to the spin susceptibility of the carrier liquid χ_s . Like other thermodynamic quantities, ρ_s does not exhibit any critical behavior at the MIT. However, ρ_s exhibits large space fluctuations at criticality, which will result in local fluctuations of magnetic properties. The quantitative renormalization of ρ_s by disorder will depend on its microscopic nature, for instance, on the degree of compensation. The enhancement of ρ_s by the carrier-carrier interactions can be described by the Fermi-liquid parameter A_F , $\rho_s \rightarrow A_F \rho_s$.³² The value of $A_F = 1.2$, as evaluated³⁴ by the local-spin-density approximation for the relevant

hole concentrations, has been adopted for our computations. We note that disorder-modified carrier-carrier interactions in the triplet particle-hole channel tend to enhance A_F , which may even drive the system towards a Stoner-like instability.³⁵ In magnetic systems, however, spin-flip scattering by fluctuations of magnetization makes this enhancement mechanism rather inefficient.

The two-fluid model is consistent with the recent EPR results,³⁶ which point the coexistence of the neutral Mn acceptors and ionized Mn d^5 states in some range of Mn concentration. Furthermore, the observed^{37,38} sign of magnetic circular dichroism in (Ga,Mn)As suggests the presence of the Fermi-liquid like states on the both sides of the MIT, as we shall discuss in Sec. IV D.

C Valence band structure and exchange splitting of the hole subbands

Since the valence band originates merely from the anion p and cation d wave functions, the exchange interaction mediated by the holes is expected to be strongly affected by anisotropy of hole dynamics and the coupling between the spin and orbital orbit degrees of freedom. To take those effects into account, the hole dispersion and wave functions are computed by diagonalizing the 6x6 Kohn-Luttinger kp matrix.³⁹ In this model, four Γ_8 and two Γ_7 bands are taken explicitly into account, whereas other bands are included by second order perturbation theory. The model is developed for zincblende and wurzite semiconductors. It allows for warping, quantizing magnetic fields, and biaxial strain but no terms associated with the lack of the symmetry inversion are taken into account. The effect of the spin-dependent interaction between the holes and the Mn spins is described in terms of the virtual-crystal and molecular-field approximations,⁴⁰ so that

$$H_{pd} = \beta s \mathbf{M}(\mathbf{r}) / g \mu_B, \quad (1)$$

where $\mathbf{M}(\mathbf{r})$ is the magnetization of the localized spins that carry magnetic moment $-Sg\mu_B$, where $S = 5/2$ and $g = 2.0$.

The explicit form of the kp 6x6 matrices, together with the matrix H_{pd} derived by us in the Luttinger-Kohn representation for arbitrary directions of magnetization \mathbf{M} , are displayed in Appendix A. We note that for the case under consideration, involving large exchange interaction and high kinetic energy, particularly important are off diagonal terms describing the p-d coupling between the Γ_8 and Γ_7 bands. A numerical procedure that serves to determine the concentration, free energy, wave functions, and optical characteristics of the holes is outlined in Appendix B. The adopted values of the Luttinger parameters γ_i and the spin-orbit splittings Δ_o are summarized in Appendix C for various III-V and II-VI parent compounds. According to photoemission studies²⁴ $\beta N_o = -1.2 \pm 0.2$ eV for (Ga,Mn)As. The

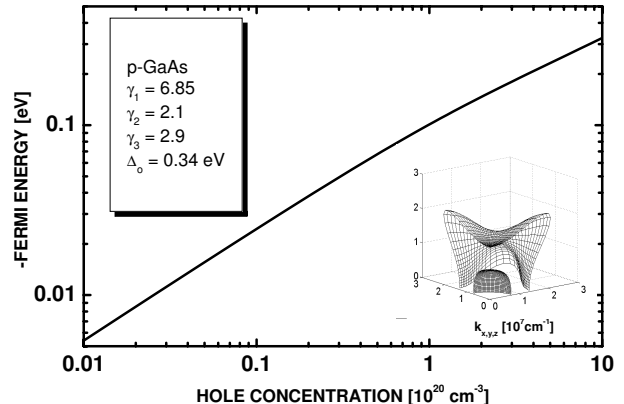


FIG. 1: Fermi energy as a function of the hole concentration p computed from the 6x6 Luttinger model for kp parameters displayed in the figure. Inset shows cross section of the Fermi sphere for $p = 3.5 \times 10^{20} \text{ cm}^{-3}$.

value $\beta N_o = -1.2$ eV is taken for the computations, though future works may reveal some dependence of β of Eq. (1) on Mn and/or hole concentrations because of energetic proximity of the Fermi and relevant Mn d-levels. Such a dependence could result also from corrections to the virtual-crystal and molecular-field approximations if a short-range part of the Mn potential is attractive for the valence band hole.²²

Figure 1 presents the dependence of the low temperature Fermi energy ε_F on the hole concentration p computed for the band parameters corresponding to GaAs. No effects of p-d exchange, disorder, or Coulomb interactions between the holes are taken into account. The corresponding density-of-states (DOS) effective mass increases from $0.67m_o$ in the limit of small hole concentrations to the value of $1.35m_o$ for $p = 5 \times 10^{20} \text{ cm}^{-3}$. This increase is caused by the kp interaction between the Γ_8 and Γ_7 bands, which—because of a relatively small magnitude of Δ_o in GaAs—is important for the relevant hole densities. The inset to Fig. 1 shows the cross section of the Fermi surface for $p = 3.5 \times 10^{20} \text{ cm}^{-3}$, which corresponds to $\varepsilon_F = -195$ meV in respect to energy of the Γ_8 point. Two valleys, the heavy and light hole subbands, are visible.

A strong and complex influence of the p-d interaction and strain upon the valence band is shown in Fig. 2. The cross sections of the Fermi spheres are depicted for $p = 3.5 \times 10^{20} \text{ cm}^{-3}$, which now corresponds to $\varepsilon_F \approx -165$ meV, and for the parameter of the exchange splitting,

$$B_G = A_F \beta M / 6g\mu_B, \quad (2)$$

taken as $B_G = -30$ meV. If $\beta N_o = -1.2$ eV and $A_F = 1.2$, this magnitude of B_G occurs for the saturation value of magnetization M at $x = 0.05$. We note at this point that some of the effects, e.g., the direction of spin-

polarization vector depends on the sign of β and thus B_G , whereas others, like the Curie temperature, are proportional to β^2 . In the absence of strain, $\epsilon = 0$, the four fold degeneracy at the Γ point is lifted by the p-d exchange, and the corresponding energies at $k = 0$ are $\pm 3B_G$ and $\pm B_G$ for $\Delta_o \gg |B_G|$. However, the splitting at non-zero wave vectors depends on the relative orientation of \mathbf{M} and \mathbf{k} .⁴⁰ In particular, since the spin of the heavy hole is polarized along \mathbf{k} for $\epsilon = 0$, the exchange splitting is seen to vanish for $\mathbf{k} \perp \mathbf{M}$. This mixing of orbital and spin degrees of freedom, together with highly nonparabolic, anisotropic, and mutually crossing dispersion relations constitute important aspects of the hole-mediated ferromagnetism in tetrahedrally coordinated semiconductors.

III. HOLE-INDUCED FERROMAGNETISM IN SEMICONDUCTORS

A Short-range antiferromagnetic superexchange and ferromagnetic double exchange

In addition to the interaction between the carriers and localized spins, the p-d hybridization leads also to the superexchange, a short-range antiferromagnetic coupling between the Mn spins. The superexchange is mediated by spin-polarization of occupied electron bands, in contrast to the Zener ferromagnetic exchange which is mediated by spin-polarization of the carrier liquid. The antiferromagnetic exchange dominates in undoped II-VI semiconductors,²⁶ and also in a compensated $\text{Ga}_{1-x}\text{Mn}_x\text{As:Sn}$.⁴¹ In order to take the influence of this interaction into account, it is convenient to parameterize the dependence of magnetization on the magnetic field in the absence of the carriers, $M_o(H)$, by the Brillouin function B_S according to

$$M_o(H) = g\mu_B S N_o x_{eff} B_S[g\mu_B H/k_B(T + T_{AF})], \quad (3)$$

where two empirical parameters, the effective spin concentration $x_{eff}N_o < xN_o$ and temperature $T_{eff} > T$, take the presence of the superexchange interactions into account.^{26,42} The dependencies $x_{eff}(x)$ and $T_{AF}(x) \equiv T_{eff}(x) - T$ are known^{43,42} for II-VI compounds.

In order to elucidate the effect of doping on x_{eff} and T_{AF} we refer to the two-fluid model described in Sec. II B. In terms of that model the delocalized or weakly localized holes account for the ferromagnetism. Actually, the participation of the same set of holes in both charge transport and the ferromagnetic interactions is shown, in $(\text{Ga,Mn})\text{As}$ ¹⁴ and in $(\text{Zn,Mn})\text{Te}$,⁴⁴ by the agreement between the temperature and field dependencies of the magnetization deduced from the extraordinary Hall effect, M_H , and from direct magnetization measurements, M_D , particularly in the vicinity of T_C . However, below T_C and in the magnetic fields greater than the coercive force, while M_H saturates (as in standard ferromagnets), M_D continues to rise with the magnetic field.^{14,38} Since

M_H is proportional to spin polarization of the carriers, its saturation may reflect a saturation of hole polarization, which—for appropriately low values of the Fermi energy—can occur even if the Mn spins are not totally spin polarized (half metallic case). It appears, however, that Mn spins in the regions depleted from the carriers (which, therefore, do not participate in the long range magnetic order) contribute also to a slowly increasing component of $M_D(H)$.

According to the two fluid model, part of the carriers are trapped on strongly localized impurity states, and thus form bound magnetic polarons (BMP). If there is an exchange coupling between the two fluids, the BMP participate in the formation of the ferromagnetic order. Furthermore, the coupling between the BMP appears to be ferromagnetic, at least in some range of relevant parameters.^{45,46} To gain the Coulomb energy, the BMP are preferentially formed around close pairs of ionized acceptors. In the case of III-V materials this leads, *via* Zener's double exchange,⁴⁷ to a local ferromagnetic alignment of neighbor Mn d^5 negative ions,⁴⁸ so that $x \approx x_{eff}$ and $T_{AF} \approx 0$. By contrast, in II-VI compounds, for which acceptor cores do not carry any spin and the degree of compensation is low, BMP are not preferentially formed around Mn pairs, so that the close pairs remained antiferromagnetically aligned, even in p-type samples. The presence of a competition between the ferromagnetic and antiferromagnetic interactions in II-VI compounds, and its absence in III-V materials, constitutes the important difference between those two families of magnetic semiconductors.

B Zener model of ferromagnetic interactions mediated by free carriers

As mentioned above, we assume that weakly localized or delocalized holes mediate long-range ferromagnetic interaction between the spins. Zener⁴⁷ first proposed a model of ferromagnetism driven by the exchange coupling of the carriers and the localized spins. According to that model, spin-polarization of the localized spins leads to spin-splitting of the bands, which results in the lowering of the carrier energy. At sufficiently low temperature, this lowering overcompensates the increase of the free energy caused by a decrease of entropy, which is associated with the polarization of the localized spins. However, the Zener model was later abandoned, as neither the itinerant character of the magnetic electrons nor the quantum (Friedel) oscillations of the electron spin-polarization around the localized spins were taken into account, both of these are now established to be critical ingredients for the theory of magnetic metals. In particular, a resulting competition between ferromagnetic and antiferromagnetic interactions in metals leads rather to a spin-glass than to a ferromagnetic ground state. In the case of semiconductors, however, the mean distance between the carriers is usually much greater than that

between the spins. Under such conditions, the exchange interaction mediated by the carriers is ferromagnetic for most of the spin pairs, which reduces the tendency towards spin-glass freezing. Actually, for a random distribution of the localized spins, the mean-field value of the Curie temperature T_C deduced from the Zener model is equal to that obtained from the Ruderman, Kittel, Kasuya, and Yosida (RKKY) approach,^{32,33,51,52} in which the presence of the Friedel oscillations is explicitly taken into account.

C Mean-field model of Curie temperature and thermodynamic properties

As reported elsewhere,⁸ the Zener model describes correctly the experimental values of T_C in both (Ga,Mn)As and (Zn,Mn)Te, provided that band structure effects are taken into account. The starting point of the model is the determination how the Ginzburg-Landau free-energy functional F depends on the magnetization M of the localized spins. The hole contribution to F , $F_c[M]$ is computed by diagonalizing the 6x6 Kohn-Luttinger matrix together with the p-d exchange contribution, and by the subsequent computation of the partition function Z , as described in Appendix B. This model takes the effects of the spin-orbit interaction into account, a task difficult technically within the RKKY approach, as the spin-orbit coupling leads to non-scalar terms in the spin-spin Hamiltonian. Moreover, the indirect exchange associated with the virtual spin excitations between the valence subbands, the Bloembergen-Rowland mechanisms,²⁶ is automatically included. The remaining part of the free energy functional, that of the localized spins, is given by

$$F_S[M] = \int_0^M dM_o H(M_o), \quad (4)$$

where $H(M_o)$ is given in Eq. (3). By minimizing $F[M] = F_c[M] + F_S[M]$ with respect to M at given T , H , and hole concentration p , one obtains $M(T, H)$ as a solution of the mean-field equation,

$$M = \mu_g \mu_B S N_o x_{eff} B_S \left[\frac{g \mu_B (-\partial F_c[M] / \partial M + H)}{k_B (T + T_{AF})} \right]. \quad (5)$$

Near the Curie temperature T_C , where M is small, we expect $F_c[M] - F_c[0] \sim M^2$. It is convenient to parameterize this dependence by a spin density-of-states ρ_s ,

$$F_c[M] = F_c[0] - A_F \rho_s \beta^2 M^2 / 2 (2g\mu_B)^2. \quad (6)$$

The spin density-of-states ρ_s is related to carrier magnetic susceptibility according to $\chi = A_F (g^* \mu_B)^2 \rho_s / 4$ and, in general, has to be determined numerically by computing $F_c[M]$. By expanding $B_S(M)$ we arrive to,

$$T_C = x_{eff} N_o S(S+1) \beta^2 A_F \rho_s(T_C) / 12 k_B - T_{AF}. \quad (7)$$

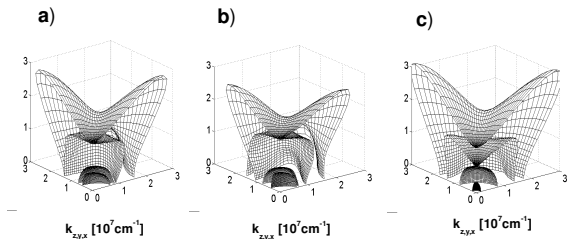


FIG. 2: Cross sections of the Fermi spheres for saturation value of magnetization M in $\text{Ga}_{0.95}\text{Mn}_{0.05}\text{As}$ with hole concentration $p = 3.5 \times 10^{20} \text{ cm}^{-3}$. Results for various orientations of magnetization \mathbf{M} and biaxial strains ϵ_{xx} are shown: (a) $M \parallel [100]$; $\epsilon_{xx} = 0$. (b) $M \parallel [100]$; $\epsilon_{xx} = -2\%$. (c) $M \parallel [001]$; $\epsilon_{xx} = +2\%$. A strong dependence of the splitting on the relative orientation of the wave vector and magnetization is visible.

For a strongly degenerate carrier liquid $-\varepsilon_F / k_B T \gg 1$, as well as neglecting the spin-orbit interaction, ρ_s becomes equal to the total density-of-states ρ for intra-band charge excitations, where $\rho = m_{DOS}^* k_F / \pi^2 \hbar^2$.

In order to check the quantitative significance of carrier entropy, the computed values of T_C were compared to those obtained assuming strong degeneration of the carrier liquid. As shown in Fig. 3 such an assumption leads to error smaller than 1% if $\varepsilon_F / k_B T > 10$. Thus, in this range, the carrier energy, not free energy, was used for the evaluation of T_C . Furthermore, we take $x_{eff} = x$ and $T_{AF} = 0$, as discussed above.

The values of T_C as a function of the hole concentration p for $\text{Ga}_{0.95}\text{Mn}_{0.05}\text{As}$, as computed by our model, are shown by the solid line in Fig. 4. Since the magnitude of T_C is directly proportional to $x_{eff} N_o \beta^2 A_F$, the theoretical results can be easily extended to other values of x , β or A_F . In particular, $T_C = 300 \text{ K}$ is expected for $x = 0.125$ and $p = 3.5 \times 10^{20} \text{ cm}^{-3}$.

D Validity of the model and comparison to other approaches

Equation (7) with $\rho_s = \rho$, that is neglecting effects of the spin-orbit interaction, has already been derived by a number of equivalent methods.^{26,32,33,34} In the present work $F_c[M]$, which served to determine T_C , $M(T, H)$, anisotropy fields, and optical spectra was obtained from the 6x6 kp model, as described in Appendices A and B. In order to illustrate the importance of band structure

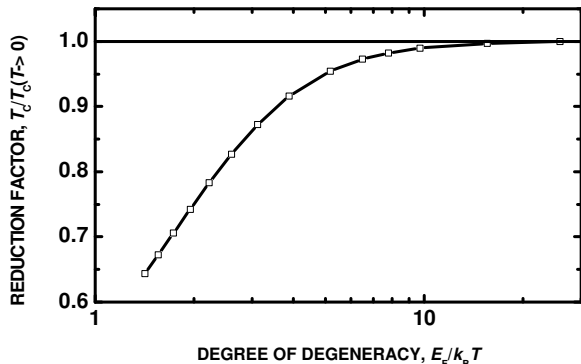


FIG. 3: The computed ratio the actual Curie temperature T_C to that obtained assuming that the hole liquid is strongly degenerate as a function of the degeneration factor.

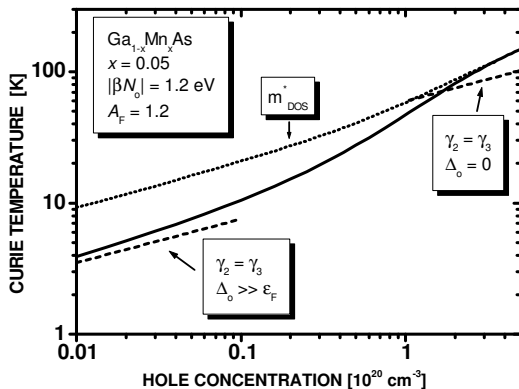


FIG. 4: Curie temperature as a function of the hole concentration for $\text{Ga}_{0.95}\text{Mn}_{0.05}\text{As}$ computed from the 6x6 Luttinger model (solid line). Straight dashed lines represent results obtained assuming a large and small value of the spin-orbit splitting Δ_o , respectively. The dotted line is calculated neglecting the effect of the spin-orbit interaction on the hole spin susceptibility.

effects, the evaluation of T_C has been performed employing various models. The two straight dashed lines in Fig. 4 depict the expected $T_C(p)$ if the warping is neglected ($\gamma_2 = \gamma_3$) as well as a large and small spin-orbit splitting $E_{\Gamma_8} - E_{\Gamma_7} \equiv \Delta_o$ is assumed, respectively. We see that the above assumptions are approximately fulfilled in low and high concentration range, respectively, but the calculation within the full model is necessary in the experimentally relevant region of the intermediate hole densities. In particular, 4x4 model^{44,49} ($\Delta_o \gg |\varepsilon_F|$) would be reasonably correct for $(\text{Zn,Mn})\text{Te}$, where Δ_o is about 1 eV but not for $(\text{Ga,Mn})\text{As}$, for which Δ_o is almost three times smaller. Finally, the dotted line shows T_C evaluated replacing ρ_s by ρ . We see that $\rho \approx \rho_s$ already for $p \approx 10^{20} \text{ cm}^{-3}$, despite that $|\varepsilon_F|$ is still two times smaller than Δ_o . In contrast, ρ_s is more than two times smaller than ρ in the limit of small p . This reduction of the spin susceptibility, and thus of T_C , stems from the absence of the exchange splitting of the heavy hole subband for $\mathbf{k} \perp \mathbf{M}$.

As described above, T_C can be computed by minimizing the free energy, and without referring to the explicit form of the Kohn-Luttinger amplitudes $u_{i\mathbf{k}}$. Since near T_C the relevant magnetization M is small, the carrier free energy, and thus T_C , can also be determined from the linear response theory. The corresponding ρ_s assumes the standard form

$$\rho_s = \lim_{q \rightarrow 0} 8 \sum_{ij\mathbf{k}} \frac{|\langle u_{i,\mathbf{k}} | s_M | u_{j,\mathbf{k}+\mathbf{q}} \rangle|^2 f_i(\mathbf{k}) [1 - f_j(\mathbf{k} + \mathbf{q})]}{E_j(\mathbf{k} + \mathbf{q}) - E_i(\mathbf{k})}, \quad (8)$$

where s_M is the component of spin operator along the direction of magnetization and $f_i(\mathbf{k})$ is the Fermi-Dirac distribution function for the i -th valence band subband. The equivalence of ρ_s as given by Eqs. (6) and (8) can be checked for the 4x4 spherical model by using the explicit form⁵⁰ of $E_i(k)$ and u_i . Such a comparison demonstrates that almost a 30% contribution to T_C originates from interband polarization.

It is straightforward to generalize the model for the case of the carriers confined to the d -dimensional space.^{32,33,52} The tendency towards the formation of spin-density waves in low-dimensional systems^{33,53} as well as possible spatial correlation in the distribution of the magnetic ions can also be taken into account. The mean-field value of the critical temperature T_q , at which the system undergoes the transition to a spatially modulated state characterized by the wave vector \mathbf{q} , is given by the solution of the equation,

$$\beta^2 A_F(\mathbf{q}, T_q) \rho_s(\mathbf{q}, T_q) \int d\zeta \chi_o(\mathbf{q}, T_q, \zeta) |\phi_o(\zeta)|^4 = 4g^2 \mu_B^2. \quad (9)$$

Here \mathbf{q} spans the d -dimensional space, $\phi_o(\zeta)$ is the envelope function of the carriers confined by a $(3-d)$ -dimensional potential well $V(\zeta)$; g and χ_o denote the Landé factor and the \mathbf{q} -dependent magnetic susceptibility of the magnetic ions in the absence of the carriers, re-

spectively. Within the mean-field approximation (MFA), such magnetization shape and direction will occur in the ordered phase, for which the corresponding T_q attains the highest value. A ferromagnetic order is expected in the three dimensional (3D) case, for which a maximum of $\rho_s(\mathbf{q})$ occurs at $q = 0$.

Since within the MFA the presence of magnetization fluctuations is neglected, our model may lead to an overestimation of the magnitude of M , and thus of T_C . To address this question we recall that the decay of the strength of the carrier-mediated exchange interaction with the distance between the spins r is described by the RKKY function, which in the 3D situation assumes the form,^{33,51,52}

$$J(r) \sim [\sin(2k_F r) - 2k_F r \cos(2k_F r)] / (2k_F r)^4. \quad (10)$$

In the case of semiconductors an average distance between the carriers $r_c = (4\pi p/3)^{-1/3}$ is usually much greater than that between the spins $r_S = (4\pi x N_o/3)^{-1/3}$. This means that the carrier-mediated interaction is ferromagnetic and effectively long range for most of the spins as the first zero of the RKKY function occurs at $r \approx 1.17r_c$. A theoretical study⁵⁴ of critical exponents for a d -dimensional space showed that as long as $\sigma < d/2$ in the dependence $J(r) \sim 1/r^{d+\sigma}$, the mean-field approach to the long wavelength susceptibility $\chi(T)$ is valid, a conclusion not affected presumably by disorder in the spin distribution. At the same time, both relevant length scale r_c , not r_S , and the critical exponents⁵⁴ $\eta = 2 - \sigma$ and $\nu = 1/\sigma$, point to much faster decay of $\chi(q)$ with q than that expected from the classical Ornstein-Zernike theory.⁵⁵ This indicates that the MFA should remain valid down to at least $|T - T_C|/T_C \approx r_S/r_c \ll 1$. Actually, the decay of $\chi(q)$ with q in the range $0 < q < 2k_F$ is corroborated by the observation of smaller critical scattering of the holes by magnetization fluctuations than that calculated for $\chi(q) = \chi(0)$.¹⁷

Recently, Monte-Carlo studies of carrier-mediated ferromagnetism in semiconductors have been initiated.^{56,57} Such an approach has a potential to test the accuracy of the MFA and to determine the actual spin configuration corresponding to the ground state. Preliminary results appear to confirm the validity of the MFA^{56,57} as well as to indicate a possibility of the existence of non-collinear magnetic structures in low-dimensional systems.⁵⁷ Another significant recent development⁵⁸ is the examination of spin-wave excitations, their spectrum and effect on magnetization. A strong reduction of T_C was predicted,⁵⁸ though it should be noted that the spin wave approximation breaks usually down at criticality. In contrast, such an approach offers valid results at low temperatures, provided that effects of magnetic anisotropy are thoroughly taken into account. Furthermore, the existence of ferromagnetic ground state was confirmed by *ab initio* total energy computations for magnetic III-V compounds.^{28,59,60} However, to what extent the employed procedures have been capable to capture accu-

rately correlation effects on the open d-shells seems to be unclear by now.

Finally, we would like to stress once more that if concentrations of the carriers and the spins become comparable, $r_c \leq r_S$, randomness associated with the competition of ferromagnetic and antiferromagnetic interactions can drive the system towards a spin-glass phase.⁶¹ In the case of II-VI compounds, the antiferromagnetic component is additionally enlarged by the superexchange interaction.⁴⁴ Furthermore, scattering by ionized impurities, and the associated non-uniform distribution of carriers in semiconductors near the MIT, may enhance disorder effects even further. We note also that in the extreme case, $r_c \ll r_S$, the Kondo effect, that is dynamic screening of the localized spins by the sea of the carriers may preclude both ferromagnetic and spin-glass magnetic ordering.

IV. COMPARISON OF THEORETICAL AND EXPERIMENTAL RESULTS FOR (GA,MN)AS

A Curie temperature and spontaneous magnetization

The most interesting property of $\text{Ga}_{1-x}\text{Mn}_x\text{As}$ epilayers is the large magnitude of T_C , up to 110 K for the Mn concentration $x = 5.3\%$.^{2,7} Because of this high T_C , the spin-dependent extraordinary contribution to the Hall resistance R_H persists up to 300 K, making an accurate determination of the hole density difficult.^{7,14,15,16} However, the recent measurement⁶² of R_H up to 27 T and at 50 mK yielded an unambiguous value of $p = 3.5 \times 10^{20} \text{ cm}^{-3}$ for the metallic $\text{Ga}_{0.947}\text{Mn}_{0.053}\text{As}$ sample, in which $T_C = 110 \text{ K}$ is observed.⁷ The above value of p is about three times smaller than xN_o , confirming the importance of compensation in (Ga,Mn)As. As shown in Fig. 4, the numerical results lead to $T_C = 120 \text{ K}$ for $x = 0.05$, and thus, $T_C = 128 \text{ K}$ for $x = 0.053$ and $p = 3.5 \times 10^{20} \text{ cm}^{-3}$. We conclude that the proposed model describes, with no adjustable parameters, high values of T_C found in (Ga,Mn)As. Furthermore, scaling theory of electronic states near the MIT, discussed in Sec. II B, makes it possible to explain the presence of the ferromagnetism on the both sides of the MIT, and a non-critical evolution of T_C across the critical point.⁷ A comparison between theoretical and experimental data in a wider range of Mn and hole concentrations requires reliable information on the hole density in particular samples, which is not presently available in the case of (Ga,Mn)As.

In the case of (Zn,Mn)Te:N, the hole concentration can readily be determined by the Hall effect measurements at 300 K.^{4,44} The absence of the extraordinary Hall effect at 300 K stems from the much lower values of T_C , $0.75 \leq T_C \leq 2.4 \text{ K}$ for $5\% \geq x \geq 2\%$ and $10^{19} \leq p \leq 10^{20} \text{ cm}^{-3}$. The model in question explains satisfactorily⁴⁴ $T_C(x, p)$. Three effects conspire to make T_C much greater in p-(Ga,Mn)As than in p-(Zn,Mn)Te at given p and x .

First, as already mentioned, the small value of the splitting Δ_o makes the reduction of T_C by spin-orbit coupling of minor importance in the case of (Ga,Mn)As. Second, because of a smaller lattice parameter, the product βN_o is greater in (Ga,Mn)As. Finally, ferromagnetic double-exchange between closely lying pairs of Mn ions is stronger than antiferromagnetic superexchange in compensated (Ga,Mn)As. In contrast, antiferromagnetic superexchange remains significant in p-(Zn,Mn)Te, as the Mn atoms are electrically inactive in II-VI compounds.

Important characteristics of ferromagnets are the magnitude and temperature dependence of the spontaneous magnetization M below T_C . Experimental studies of metallic samples indicates that on lowering temperature M increases as the Brillouin function reaching the saturation value M_s for $T \rightarrow 0$.⁷ This behavior indicates that a molecular field H^* acting on the Mn spins is proportional to their magnetization M . Figure 5 presents values of M/M_s as a function of T/T_C calculated with no adjustable parameter for (Ga,Mn)As containing various hole and Mn concentrations. We see that indeed the computed Mn spin magnetization $M(T)/M_s$ follows, to a good approximation, the Brillouin function, except for materials with rather small values p or large values of x . The latter cases correspond to the half-metallic situation, for which only the ground-state hole subband is populated even at $M < M_s$, so that the molecular field produced by the carriers H^* attains its maximum value and, therefore, ceases to be proportional to M . Nevertheless, the saturation value M_s can be reached provided that temperature is sufficiently low, $k_B T_{eff} \ll Sg\mu_B H^*$. Such a half-metallic behavior is observed in the case of ferromagnetic correlation imposed by a dilute hole liquid in (Cd,Mn)Te quantum wells.⁵³

B Hole magnetization and spin polarization

The magnitude of magnetization presented in the previous section was computed neglecting a possible contribution originating from hole magnetic moments. Such a contribution can be significant as the hole liquid is spin-polarized for non-zero magnetization of the Mn spins. Because of the spin-orbit interaction, the hole magnetization consists of two components. One comes from magnetic moments of the hole spins, described by the Landé factor of the free electrons and the Luttinger parameter κ . Another contribution, absent for localized carriers, originates from diamagnetic currents, whose magnetic moments can be oriented along the spin polarization by the spin-orbit interaction. The evaluation of the latter requires the inclusion of the Landau quantization in the kp hamiltonian. The carrier magnetization M_c is then given by,

$$M_c = - \lim_{T, H \rightarrow 0} \partial G_c(H) / \partial H, \quad (11)$$

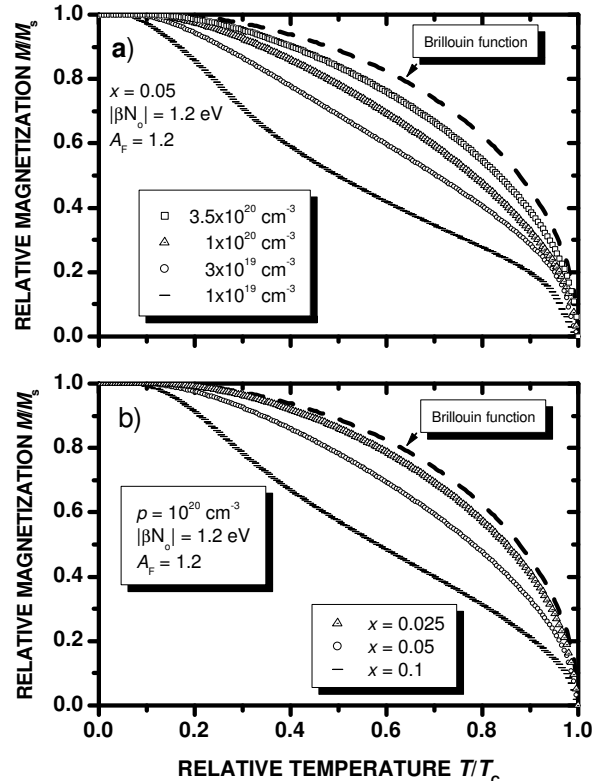


FIG. 5: The computed emerging of spontaneous magnetization M below the Curie temperature T_C for various hole concentrations p (a) and Mn contents x (b) in $\text{Ga}_{0.95}\text{Mn}_{0.05}\text{As}$ (points). If the exchange splitting of the valence band is much smaller than the Fermi energy (large p , small x), the evolution of magnetization follows the Brillouin function (dashed lines).

where the Gibbs thermodynamic potential is calculated for a given value of the Mn spin magnetization M and the Fermi energy $\varepsilon_F(M)$ as a function of the magnetic field acting on the carriers H . In general, the eigenvalue problem for the holes in the magnetic field cannot be transformed into an algebraic equation. Such a transformation is, however, possible if the warping is neglected. We have, therefore, calculated the hole magnetization M_c disregarding the anisotropy, that is assuming $\gamma_1 = 6.85$, $\gamma_2 = \gamma_3 = 2.58$, and $\kappa = 1.2$. The explicit form of the relevant Luttinger matrices is displayed in Appendix A. The partition function Z was computed by summing over the Landau index n , the wave vector k_z , and the six hole subbands.

The results of the computations are shown in Fig. 6, where M_c is plotted as a function of p for $B_G = A_F\beta M/6g\mu_B = -30$ meV. In this paper, for sake of comparison with experimental results we depict magnetization in the SI units according to $\mu_o M[\text{T}] = 4\pi 10^{-4} M[\text{emu}]$. It is seen the diamagnetic (orbital) contribution to M_c is negative and dominant. The spin term is positive, which for the antiferromagnetic sign of the p-d exchange integral β points to the negative sign of the hole Landé factor g_h . A visible decrease of the spin contribution for the large p corresponds to a cross-over to the free electron value $g = 2.0$ occurring when $|\varepsilon_F|$ approaches Δ_o . In Fig. 7, M_c is plotted versus M for various p . It is seen that for the employed values of the parameters, M_c reaches only 5% of $\mu_o M = 65$ mT, which corresponds to the saturation value of Mn magnetization for $x = 0.05$. A rather weak magnitude of M_c results from a partial compensation of the spin and orbital contributions to M_c as well as from smaller concentration and spin of the holes in comparison to those of the Mn ions. We conclude that delocalized or weakly localized holes give a minor contribution to the total magnetization. Accordingly M_c is neglected when determining the direction of easy axes and the magnitude of anisotropy fields.

In view of the on-going experiments⁶ on electrical spin injection from (Ga,Mn)As, an important question arises what is the degree of hole spin polarization \mathcal{P} as a function of p and B_G . Furthermore, \mathcal{P} appears to control the magnitude of the extraordinary Hall effect. It is, therefore, interesting to determine conditions, under which the usual assumption about the linear relation between \mathcal{P} and magnetization of the Mn spins M is fulfilled.

The contribution of all four hole subbands to the Fermi cross section visible in Fig. 2 indicates that the exchange splitting is too small to lead to the total spin polarization for $p = 3.5 \times 10^{20} \text{ cm}^{-3}$ and $x = 0.05$ ($|B_G| = 30$ meV). Furthermore, a destructive effect of the spin-orbit interaction on the magnitude of \mathcal{P} can be expected. In order to evaluate $\mathcal{P} \equiv 2\langle s_M \rangle / p$ we note that according to Eq. (1),

$$\mathcal{P} = \frac{2g\mu_B}{\beta p} \frac{\partial F_c(M)}{\partial M}. \quad (12)$$

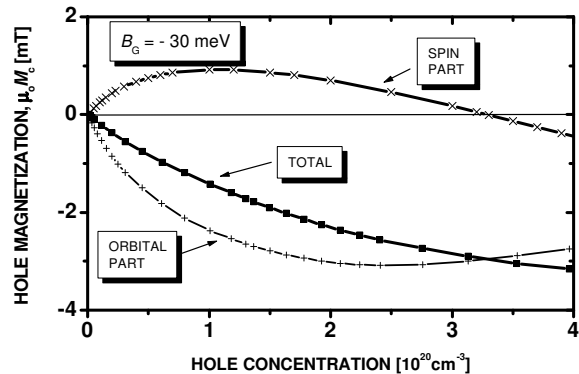


FIG. 6: Magnetization M_c of the hole liquid (squares) in $\text{Ga}_{1-x}\text{Mn}_x\text{As}$ computed as a function of the hole concentration for the spin splitting parameter $B_G = -30$ meV (the latter corresponds to the saturation value of Mn spin magnetization M for $x = 0.05$). Crosses show spin and orbital contribution to M_c .

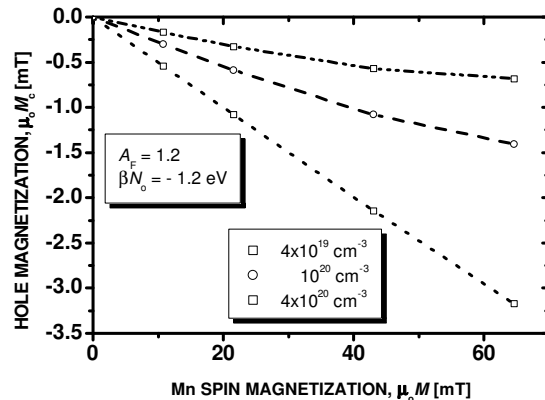


FIG. 7: Computed hole magnetization M_c as a function of Mn spin magnetization M for various hole concentrations in $\text{Ga}_{1-x}\text{Mn}_x\text{As}$.

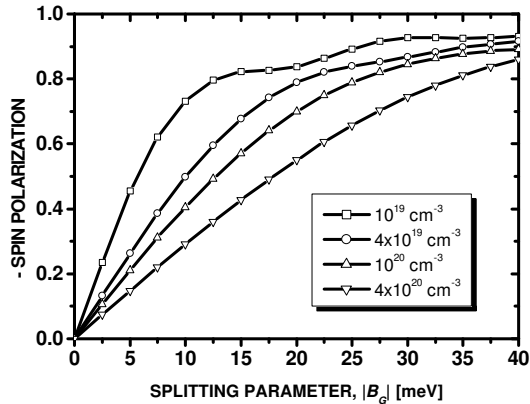


FIG. 8: Computed degree of spin polarization of the hole liquid as a function of the spin splitting parameter for various hole concentrations in $\text{Ga}_{1-x}\text{Mn}_x\text{As}$ ($B_G = -30$ meV corresponds to the saturation value of Mn spin magnetization for $x = 0.05$). The polarization of the hole spins is oriented in the opposite direction to the polarization of the Mn spins.

Figure 8 presents the dependence of \mathcal{P} on B_G for the experimentally relevant range of p . We see that $|\mathcal{P}|$ tends to saturate with $|B_G|$, and thus with M . This means that for large values of the splitting B_G , magnetization M evaluated from the extraordinary Hall effect is underestimated. At the same time, the calculation demonstrates that despite the spin-orbit interaction $|\mathcal{P}|$ becomes greater than 0.8 for $3|B_G| > |\varepsilon_F|$. This is due to the fact that the redistribution of the holes over the spin subbands occurs in the way which maximizes the gain of the exchange energy, and thus the magnitude of $|\mathcal{P}|$. This in contrast to the case $|\varepsilon_F| \gg |B_G|$, for which the spin polarization is reduced by a factor greater than two from the value corresponding to the absence of the spin-orbit coupling at low hole concentrations. We also note that because of the antiferromagnetic character of the p-d coupling ($\beta N_o < 0$), the polarization of the hole spins is oriented in the opposite direction than the polarization of the Mn spins.

C Easy axis and anisotropy field

Already early studies of a ferromagnetic phase in (Ga,Mn)As epilayers demonstrated the existence of substantial magnetic anisotropy.⁶³ Magnetic anisotropy is usually associated with the interaction between spin and orbital degrees of freedom of the *magnetic* electrons. According to the model in question, these electrons are in the d^5 configuration. For such a case the orbital momentum $L = 0$, so that no effects stemming from the spin-orbit coupling are to be expected. To reconcile the

model and the experimental observations, we note that the interaction between the localized spins is mediated by the holes, characterized by a non-zero orbital momentum. An important aspect of the present model is that it does take into account the anisotropy of the carrier-mediated exchange interaction associated with the spin-orbit coupling in the host material, an effect difficult to include within the standard approach to the RKKY interaction.

We start by considering an unstrained thin film with the [001] crystal direction perpendicular to its plane. The linear response is isotropic in cubic systems but magnetic anisotropy develops for non-zero magnetization: the hole energy depends on the orientation of M in respect to crystal axes and, because of stray field energy E_d , on the angle Θ between M and the normal to the film surface. A computation of the hole energies $E_c[M]$ for relevant parameters and [100], [110], and [111] orientations of M indicates that $E_c[M]$ can be described by the lowest order cubic anisotropy, so that, taking the stray field energy into account,⁶⁴

$$E_c(M, \Theta, \varphi) - E_c(M, \pi/2, 0) = K_d(M) \cos^2 \Theta + K_{c1}(M) (\sin^4 \Theta \sin^2 \varphi \cos^2 \varphi + \sin^2 \Theta \cos^2 \Theta), \quad (13)$$

where $K_d(M) = 2\pi M^2$. For $4K_d < -K_{c1}$ the easy axis is oriented along [111] or equivalent directions. Otherwise, as is usually the case for parameters of (Ga,Mn)As, M lies in the (001) plane, and the easy axis is directed along [100] for $K_{c1} > 0$ or along [110] (or equivalent) crystal axis in the opposite case. It turns out that the sign of K_{c1} depends on the degree of occupation the hole subbands as well as on their mixing by the p-d and kp interactions. As a result, the easy axis fluctuates between [100] and [110] as a function of p . To quantify the strength of the cubic anisotropy in (Ga,Mn)As we computed $K_{c1}(M)$, and then the minimum magnitude of an external magnetic field $H_{cu} = 2|K_{c1}/M|$ (or $\mu_o H_{cu} = 2|K_{c1}/M|$ in the SI units), which aligns the spontaneous magnetization M along the hard direction. Figure 9 shows how H_{cu}/M and the direction of the easy axis oscillates as a function of p for various $B_G = A_F \beta M / 6g\mu_B$. As expected, H_{cu} tends to zero when B_G decreases. Nevertheless, for $|B_G| = 40$ meV ($\mu_o M \approx 85$ mT), $\mu_o H_{cu}$ up to 0.2 T can be expected. Since, however, the orientation of the easy axis changes rapidly with p and B_G , intrinsic and extrinsic disorder—which leads to broadening of hole subbands—will presumably diminish the actual magnitude of magnetic anisotropy.

As shown in Fig. 2, strain has a rather strong influence on the valence subbands. It can, therefore, be expected that magnetic properties resulting from the hole-mediated exchange can be efficiently controlled by strain engineering. Indeed, sizable lattice-mismatch driven strain is known to exist in semiconductor layers. In some cases, particularly if epitaxy occurs at appropriately low temperatures, such strain can persist even beyond the critical thickness due to relatively high barriers for the formation of misfit dislocations. We evalu-

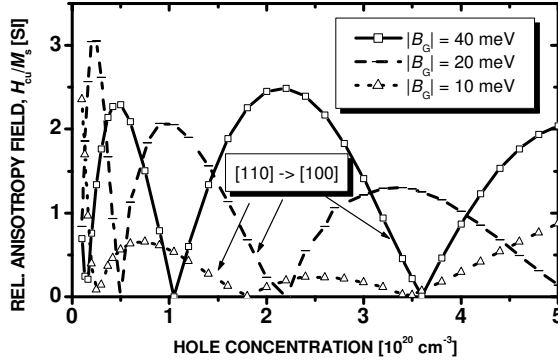


FIG. 9: Computed minimum magnetic field H_{cu} (divided by M) necessary to align magnetization M along the hard axis for cubic (unstrained) $\text{Ga}_{1-x}\text{Mn}_x\text{As}$ film. As a function of the hole concentration and the spin-splitting parameter B_G , the easy and hard axes fluctuate alternatively between $[110]$ and $[100]$ (or equivalent) directions in the plane of the film. The symbol $[110] \rightarrow [100]$ means that the easy axis is along $[110]$, so that H_{cu} is applied along $[100]$ ($B_G = -30$ meV corresponds to the saturation value of M for $\text{Ga}_{0.95}\text{Mn}_{0.05}\text{As}$).

ate the magnitude of resulting effects by using the Bir-Pikus hamiltonian,³⁹ adopted for biaxial strain, as shown in Appendix A. Three parameters control strain phenomena in the valence band: the deformation potential b , taken as $b = -1.7$ eV,⁶⁵ the ratio of elastic moduli $c_{12}/c_{11} = 0.453$,⁶⁵ and the difference between the lattice parameters of the substrate and the layer, Δa . The latter is related to relevant components of the strain tensor according to,

$$\epsilon_{xx} = \epsilon_{yy} = \Delta a/a; \quad (14)$$

$$\epsilon_{zz} = -2\epsilon_{xx}c_{12}/c_{11}. \quad (15)$$

We have found that biaxial strain has a rather small influence on T_C . In the experimentally relevant range of hole concentrations $5 \times 10^{20} > p > 10^{20} \text{ cm}^{-3}$, both tensile and compressive strain diminish T_C . The relative effect attains a maximum at $p \approx 2 \times 10^{20} \text{ cm}^{-3}$, where $[T_C(\epsilon_{xx}) - T_C(0)]/T_C(0) \approx -2.4\%$ and -4.9% for $\epsilon_{xx} = 1\%$ and -1% , respectively. However, such a strain leads to uniaxial anisotropy, whose magnitude can be much greater than that resulting from either cubic anisotropy or stray fields. The corresponding anisotropy field H_{un} assumes the form,

$$H_{un} = |2[E_c([001]) - E_c([100])]/M + 4\pi M|[\text{emu}]; \quad (16)$$

$$\mu_o H_{un} = |2[E_c([001]) - E_c([100])]/M + \mu_o M|[\text{SI}] \quad (17)$$

where the last term describes the stray-field effect. According to results of computations presented in Fig. 10,

in the region of such low hole concentrations that minority spin subbands are depopulated, the easy axis takes the $[001]$ direction for the compressive strain, while is in the (001) plane for the opposite strain. Such a behavior of magnetic anisotropy was recently noted within a 4×4 model of the valence band.⁴⁹ However, for the experimentally relevant hole concentrations and values of B_G (Figs. 10 and 11) the easy axis is oriented along $[001]$ direction for the tensile strain, whereas resides in the (001) plane for the case of unstrained or compressively strained films. This important result, announced already in our previous work,⁸ is corroborated by the experimental study,⁶³ in which either $(\text{Ga},\text{In})\text{As}$ or GaAs substrate was employed to impose tensile or compressive strain, respectively. In particular, for the $\text{Ga}_{0.0965}\text{Mn}_{0.035}\text{As}$ film on GaAs , for which $\epsilon_{xx} = -0.2\%$, the anisotropy field $\mu_o H_{un} = 0.4 \pm 0.1$ T is observed,⁶³ in quantitative agreement with the theoretical results of Fig. 11.

Finally, we mention that strong strain effects may suggest the importance of magnetostriction in the studied compounds. We have not explored this issue yet, and note that prior to its examination the question concerning the collective Jahn-Teller effect in heavily doped p-type zinc-blende semiconductors has to be addressed.

D Optical absorption and magnetic circular dichroism

In the case of II-VI diluted magnetic semiconductors, detail information on the exchange-induced spin-splitting of the bands, and thus on the coupling between the effective mass electrons and the localized spins has been obtained from magneto-optical studies.^{26,66} Similar investigations^{37,38,67,68} of $(\text{Ga},\text{Mn})\text{As}$ led to a number of surprises. The most striking was the opposite order of the absorption edges corresponding to the two circular photon polarizations in $(\text{Ga},\text{Mn})\text{As}$ comparing to II-VI materials. This behavior of circular magnetic dichroism (MCD) suggested the opposite order of the exchange-split spin subbands, and thus a different origin of the sp-d interaction in these two families of DMS. A new light on the issue was shed by studies of photoluminescence (PL) and its excitation spectra (PLE) in p-type $(\text{Cd},\text{Mn})\text{Te}$ quantum wells.^{3,53,69} It has been demonstrated that the reversal of the order of PLE edges corresponding to the two circular polarizations results from the Moss-Burstein effect, that is from the shifts of the absorption edges associated with the empty portion of the valence subbands in the p-type material. This model was subsequently applied to interpret qualitatively the magnetoabsorption data for metallic $(\text{Ga},\text{Mn})\text{As}$.³⁷ Surprisingly, however, the anomalous sign of the MCD was present also in non-metallic $(\text{Ga},\text{Mn})\text{As}$, in which EPR signal from occupied Mn acceptors was seen.³⁶ Another striking property of the MCD is a different temperature dependence of the normalized MCD at low and high photon energies in ferromagnetic $(\text{Ga},\text{Mn})\text{As}$.³⁸ This observation was taken as

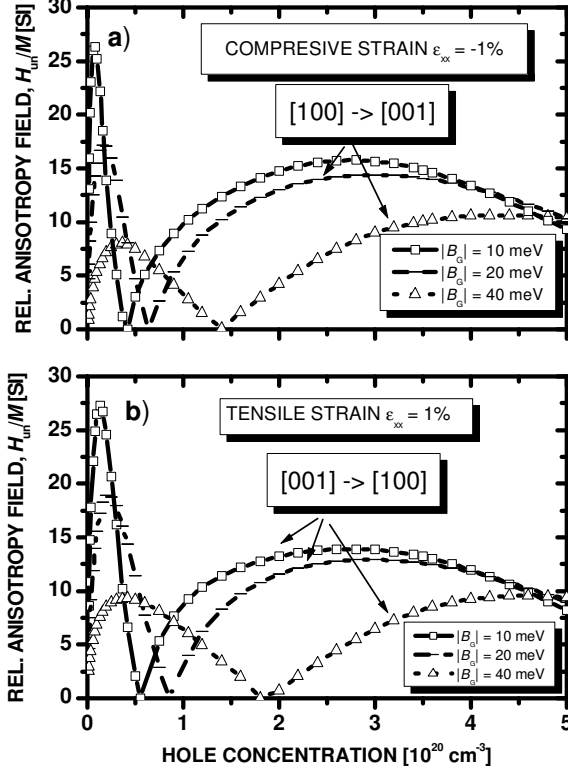


FIG. 10: Computed minimum magnetic field H_{un} (divided by M) necessary to align magnetization M along the hard axis for compressive (a) and tensile (b) biaxial strain in $\text{Ga}_{1-x}\text{Mn}_x\text{As}$ film for various values of the spin-splitting parameter B_G . The easy axis is along $[001]$ direction and in the (001) plane at low and high hole concentrations for compressive strain, respectively (a). The opposite behavior is observed for tensile strain (b). The symbol $[100] \rightarrow [001]$ means that the easy axis is along $[100]$, so that H_{un} is applied along $[001]$ ($B_G = -30$ meV corresponds to the saturation value of M for $\text{Ga}_{0.95}\text{Mn}_{0.05}\text{As}$).

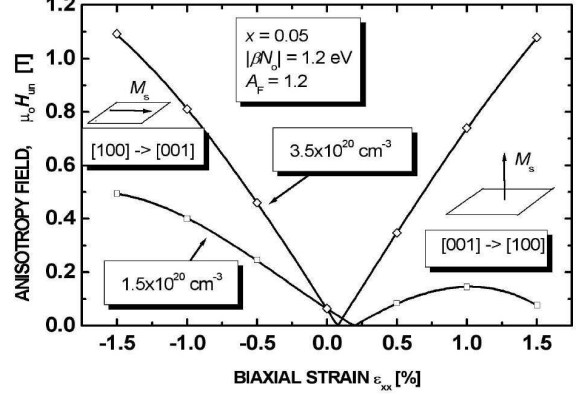


FIG. 11: Computed minimum magnetic field H_{un} necessary to align the saturation value of magnetization M_s along the hard axis as a function of biaxial strain component ϵ_{xx} for two values of the hole concentrations in $\text{Ga}_{0.95}\text{Mn}_{0.05}\text{As}$. The symbol $[100] \rightarrow [001]$ means that the easy axis is along $[100]$, so that H_{un} is applied along $[001]$.

an evidence for the presence of two spectrally distinct contributions to optical absorption.³⁸

We begin by noting that according to our two-fluid model, the co-existence of strongly and weakly localized holes is actually expected on the both sides of the MIT. Since the Moss-Burstein effect operates for interband optical transitions involving weakly localized states, it leads to the sign reversal of the MCD, also on the insulating side of the MIT. Conversely, the existence of the MCD sign reversal can be taken as an experimental evidence for the presence of the Fermi liquid-like states on the insulating side of the MIT.

In order to shed some light on those issues we calculate absorption and MCD spectra in a model that takes the complex structure of the valence band into account. The band-gap E_g is expected to depend on both Mn and hole concentration due to the alloy and band narrowing effects. To take this dependence into account as well as to include disorder-induced band tail effects⁷⁰ we assume, guided by experimental results to be discussed below, that $E_g = 1.2$ eV. Our computation of the absorption coefficient $\alpha(\omega)$ are performed according to a scheme outlined in Appendix B, taking the electron effective mass $m_e^* = 0.07m_0$, the Kane momentum matrix element $P = 9.9 \times 10^{-8}$ eVcm, and the refractive index $n_r = 3.5$. As shown in Fig. 12, contributions to α originating from particular valence bands are clearly visible. Because of the Moss-Burstein shift, the onset and the form of $\alpha(\omega)$ for particular transitions depend on the hole concentration. In particular, $\alpha(\omega)$ corresponding to the light-hole band exhibits a step-like behavior which, in the case of the heavy hole band, is broadened by warp-

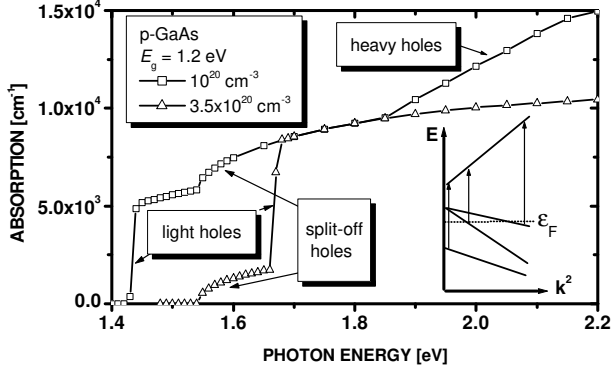


FIG. 12: Absorption edge in p-GaAs computed for two values of the hole concentrations. Inset shows three kinds of possible photon-induced transitions corresponding to particular valence subbands. Absorption edges associated with electron transitions from particular subbands are labeled.

ing. While no quantitative data on $\alpha(\omega)$ are available for (Ga,Mn)As, the computed magnitude and spectral dependence of $\alpha(\omega)$ reproduce correctly experimental results for p-GaAs.⁷¹

The influence of the sp-d band splittings on the absorption edge is shown in Fig. 13. The computation are carried out for the Faraday configuration and with the value of the s-d exchange energy $\alpha N_o = 0.2$ eV observed in II-VI semiconductors. The theoretical results confirm that the Moss-Burstein effect accounts for the sign reversal of the magnetic circular dichroism (MCD). The energy splitting of the absorption edge depends on ω but its magnitude is similar to that observed experimentally.³⁷ A detail comparison requires from one hand experimental information on the absolute values of $\alpha(\omega)$ and, on the other, more careful consideration of band tailing effects. Furthermore, contributions from intra-valence-band and from intra-d-shell transitions are expected at low and high energy wings of the absorption edge, respectively. We predict that not only the former but also the latter are substantially enlarged in p-type materials. Indeed, the empty valence band states allow for admixtures of p-like states to the localized d orbitals.

The magnetization-induced splitting of the bands is seen to lead to a large energy difference between the positions of the absorption edges corresponding to the two opposite circular polarizations. This may cause an unusual dependence of the low-energy onset of MCD on magnetization, and thus on temperature. In particular, a standard assumption about the proportionality of MCD and magnetization becomes invalid. To find out whether the latter is responsible for the anomalous temperature dependence of MCD at low photon energies,³⁸ we com-

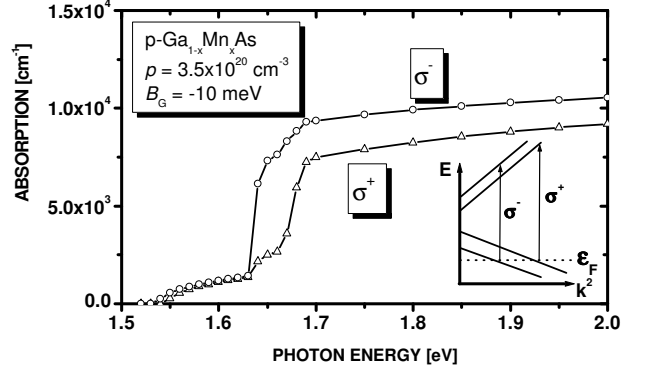


FIG. 13: Absorption edge for two circular polarizations in p-(Ga,Mn)As computed for spin-splitting parameter $B_G = -10$ meV and hole concentration $3.5 \times 10^{20} \text{ cm}^{-3}$. Inset shows how the Fermi level of the holes reverses relative positions of the edges corresponding to σ^+ and σ^- polarizations. In general, electron transitions from six valence subbands contribute to optical absorption.

pute the differential transmission coefficient that was examined experimentally³⁸

$$\Delta = (T^+ - T^-)/(T^+ + T^-). \quad (18)$$

Here T^+ and T^- are the transmission coefficients for right and left circularly polarized light. To take the effect of interference into account,³⁸ these coefficients are calculated for the actual layout of the samples, which consisted of a transparent (Ga,Al)As etching stop layer and the absorbing (Ga,Mn)As film, each 200 nm thick. The same value of the refractive index $n_r = 3.5$ are adopted for both compounds.

Figure 14 shows the ratio $\Delta(\omega)/\Delta(1.78 \text{ eV})$ computed for $p = 3.5 \times 10^{20} \text{ cm}^{-3}$ and various $B_G \sim M$. In the range of high photon energies, $\omega > 1.6$ eV, the results collapse into one curve for all values of B_G . This means that $\Delta(\omega) = M(T)f(\omega)$ in this range, where $f(\omega) \sim T^{-1}\partial T/\partial\omega$. However, in the region of the absorption edge, the dependence of Δ on B_G is by no means linear, so that the normalized values $\Delta(\omega)/\Delta(1.78 \text{ eV})$ do not follow any single curve. As seen $\Delta(\omega)/\Delta(1.78 \text{ eV})$ peaks at the greatest value the smallest B_G . This is the behavior found experimentally.³⁸ We conclude that the two observed distinct spectroscopic regions³⁸ correspond to standard band to band transitions, for which the proportionality of Δ to B_G holds, and to the onset of the absorption edge that is shifted and made more steep by the Moss-Burstein effect. Actually, the peak values of $\Delta(\omega)/\Delta(1.78 \text{ eV})$ determined numerically for the low energy region are even greater than that observed in (Ga,Mn)As,³⁸ presumably because of scattering broadening of the absorption edge, neglected in our model.

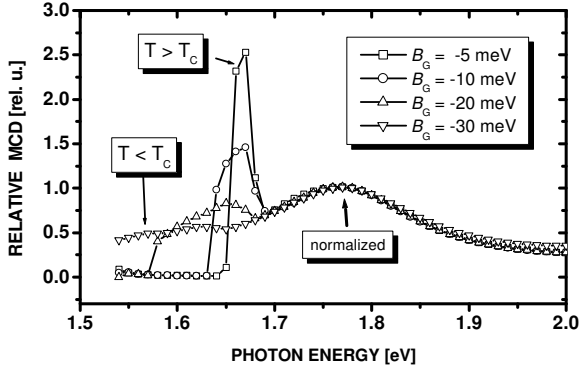


FIG. 14: Spectral dependence of magnetic circular dichroism in p-(Ga,Mn)As computed for hole concentration $3.5 \times 10^{20} \text{ cm}^{-3}$ and various spin-splitting parameters B_G . The magnitudes of MCD at given B_G are normalized by its value at 1.78 eV.

V. CHEMICAL TRENDS

A Material parameters

The ability of the present model to describe successfully various aspects of the ferromagnetism in (Ga,Mn)As as well as in (Zn,Mn)Te,^{4,8,44} has encouraged us to extend the theory towards other p-type diluted magnetic semiconductors. In this Section, we present material parameters that have been adopted for the computations presented elsewhere.⁸ We supplement also the previous results⁸ by the data for (In,Mn)N, (Cd,Mn)S, and (Cd,Mn)Se. For concreteness, we will assume that 5% of the cation sites are occupied by the Mn ions in the 2+ charge state, and that the corresponding localized spins $S = 5/2$ are coupled by the indirect exchange interaction mediated by 3.5×10^{20} holes per cm^3 . The enhancement effect of the exchange interaction among the holes is described by the Fermi liquid parameter $A_F = 1.2$. As explained in Sec. II B, no influence of the antiferromagnetic superexchange is taken into account in the case of the group III-V and IV semiconductors, in which the Mn supplies both localized spins and holes. By contrast, it is assumed that in the case of II-VI semiconductors $x_{eff} = 0.0297$ for $x = 0.05$ and $T_{AF} = 1$ K, except for (Zn,Mn)Te, where $T_{AF} = 2.9$ K,^{42,43} and (Cd,Mn)Te, for which $T_{AF} = 1.5$ K.⁷²

The values of the parameters that are used to determine chemical trends are summarized in Tables I and II for cubic and wurzite semiconductors, respectively. If no experimentally determined values are available, the effective mass parameters are determined by fitting the appropriate kp model to results of band structure computations. No lattice polaron corrections are taken into con-

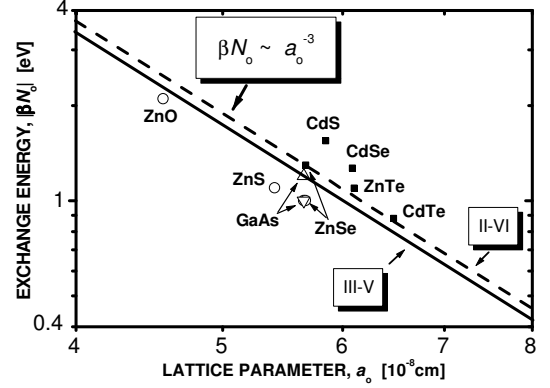


FIG. 15: Energy of p-d exchange interaction for various materials containing 5% of Mn as a function of lattice parameter. The values shown by solid squares were determined from excitonic splittings in the magnetic field,^{22,43,72,80} while the empty symbols denote values evaluated from photoemission data.^{24,77} Solid and dashed lines represent formulae adopted for the determination of the exchange energy for other materials, as shown in Tables I and II.

sideration. Since we are interested in a relatively small concentration of magnetic ions, $x = 0.05$, the effect of the Mn incorporation upon the lattice and band structure parameters is disregarded.

In the case of ZnSe, the recently determined^{73,74} values of the Luttinger parameters γ_i lead to a negative hole mass for the [110] crystallographic direction, an effect not supported by the existing theoretical studies of the valence band structure in this material.^{75,79} Accordingly, an older set⁷⁶ of γ_i had been taken for the previous calculation.⁸ The present values of γ_i are within experimental uncertainties of the current determinations⁷³ and, at the same time, lead to a good description of the computed band structure of the valence band in ZnSe.⁷⁵

In addition to the spin density of states at the Fermi level, the Curie temperature is proportional to the square of the p-d exchange integral β . Figure 15 presents the magnitudes of the exchange energy βN_o as determined by photoemission and magneto-optical studies for various DMS containing about 5% on Mn. The values of $|\beta N_o|$ are seen to increase when the lattice parameter decreases. This trend stems⁷⁷ from the corresponding changes in the charge transfer and correlation energies as well as from a dependence of the p-d hybridization energy on the bond length b .⁷⁷ It should, however, be recalled that b , in contrast to the average value of the lattice constant, does not obey the Vegard law in alloys but rather conserves the value corresponding to the end compounds.¹³

Thus, in order to obtain the values of βN_o for materials, for which no direct determination is available,

guided by the results presented in Fig. 15, we assume $\beta N_o \sim a_o^{-3}$, *i. e.*, $\beta = \text{const.}$ More explicitly, for group III-V and IV semiconductors we take

$$\beta_{III-V} = \beta(\text{GaMnAs}). \quad (19)$$

Similarly, for the II-VI materials

$$\beta_{II-VI} = \beta(\text{ZnMnSe}), \quad (20)$$

where the p-d energy $\beta N_o(\text{GaMnAs}) = -1.2 \text{ eV}$,²⁴ and $\beta N_o(\text{ZnMnSe}) = -1.3 \text{ eV}$.⁸⁰

B Curie temperatures

Figure 16 presents the calculated values of the Curie temperature T_C for III-V and II-VI semiconductors containing 5% of Mn and 3.5×10^{20} holes per cm^3 . The data for Si and Ge are also included. The most remarkable result is a strong increase of T_C for materials consisting of lighter elements. Actually, T_C exceeding room temperature is expected for GaN, InN, and ZnO for the assumed values of the Mn and hole concentrations. It has been checked for GaN that the value of T_C for the zinc-blend modification of this material is by 6% greater than that for wurzite case.

By comparing results of numerical calculations with the general Eq. (7) for T_C three interrelated mechanisms accounting for the chemical trends visible in Fig. 16 can be identified. First, the reduction of the spin density-of-states, and thus T_C by the spin-orbit interaction ceases to operate in materials with light anions. Second, the effective mass, and thus the density-of-states tend to increase for materials with stronger bonds. Finally, the smaller lattice constant at given x corresponds to the greater value of $N_o x$, density of the magnetic ions. It should be noted at this point that T_C is proportional to β^2 , assumed here to be material independent. This assumption corresponds, however, to a strong increase of $|\beta N_o|$ with decreasing lattice constant, as shown in Fig. 15.

It can be expected that the chemical trends established here are not altered by the uncertainties in the values of the relevant parameters. Our evaluations of the strength of the ferromagnetic interactions mediated by the holes is qualitatively valid for Mn, as well as for other magnetic ions, provided that two conditions are met. First, the magnetic electrons stay localized and do not contribute directly to the Fermi sphere. Secondly, the holes are delocalized and, in particular, do not form small magnetic polarons, such as Zhang-Rice singlets.²¹

VI. SUMMARY AND OUTLOOK

In this paper, theory of ferromagnetism in p-type zincblende and wurzite semiconductors containing a sizable concentration of magnetic ions has been proposed. In has

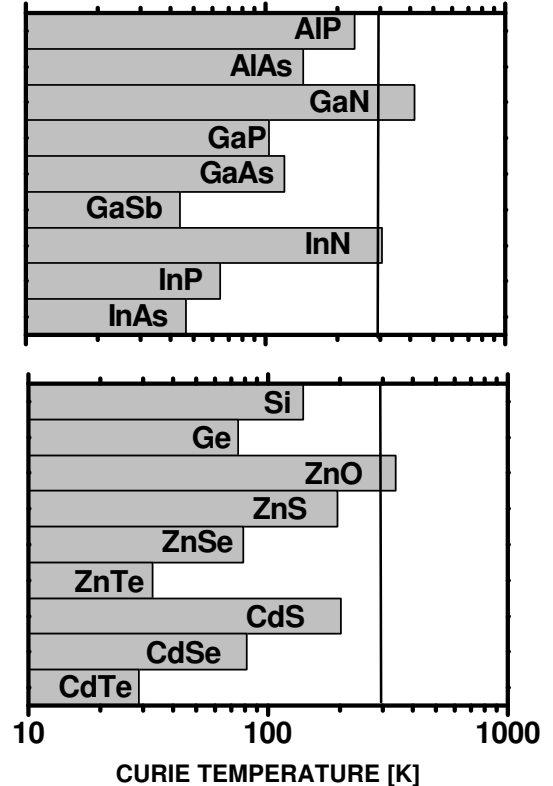


FIG. 16: Curie temperatures evaluated for various III-V (a) as well group IV and II-VI semiconducting compounds (b) containing 5% of Mn in 2+ charge state and 3.5×10^{20} holes per cm^3 . Material parameters adopted for the calculation are displayed in Tables I and II.

been argued that over the relevant range of the hole densities the ferromagnetic coupling between the localized spins is primarily mediated by delocalized or weakly localized holes residing in p-like valence band. Accordingly, particular attention has been paid to incorporate into the Zener model effects of kp and spin-orbit interactions as well as of biaxial strain. It has been demonstrated that theory describes qualitatively, and often quantitatively, a body of experimental results accumulated over the recent years for (Ga,Mn)As. In particular, Curie temperature, saturation value of magnetization, hole spin magnetization and polarization, magnetic anisotropies and magnetoelastic effects, optical absorption and magnetic circular dichroism have been interpreted.

Giant negative magnetoresistance, sharp field-induced insulator-to-metal transition,⁸¹ and a sizable increase of high frequency conductivity with the magnetic field⁸² were observed in p-(Hg,Mn)Te. Those findings were attributed to the growing participation of the light holes in transport when the p-d exchange splitting increases.^{81,82} This implies a shift of the Drude weight from high to low frequencies as a function of the valence-band splitting. Such effects, in both d.c.^{14,78} and a.c.^{83,84} conductivity have more recently been detected in (Ga,Mn)As, and can qualitatively be interpreted in the same way. This provides an additional support for our conclusion about the similarity of the mechanisms accounting for the hole-mediated exchange interaction in II-VI and III-V magnetic semiconductors. However, our work identifies also an aspect of ferromagnetism, which points to a difference between those two families of magnetic semiconductors. In the case of II-VI compounds, a short-range antiferromagnetic superexchange lowers the magnitude of T_C . This lowering appears to be much less efficient in III-V semiconductors, where the Mn ions act as acceptors, compensated partly by donor defects. Thus, the localized holes reside preferentially on the Mn pairs, so that the hole-mediated ferromagnetic coupling (a variant of Zener's double exchange) can overcompensate the antiferromagnetic superexchange.

The model put forward here has also been used to explore the expected chemical trends. It has been found that particularly large value of the Curie temperature are

expected for materials built up from light elements. Important issues of solubility limits and self-compensation need, however, to be addressed experimentally. In particular, the pinning of the Fermi energy by AX-type centers or other defects can preclude the increase of the hole concentration in many systems. High pressure research can shed some light on this issue. Since, in general, III-V compounds can easier be doped by impurities that are electrically active, whereas a large quantity of transition metals can be incorporated into II-VI materials, a suggestion has been put forward to grow magnetic III-V/II-VI short period superlattices.⁸⁵ Further numerical and experimental studies of magnetic semiconductors as well as of heavily p-doped non-magnetic systems are expected to improve our understanding of the hole-mediated ferromagnetism in zinc-blende and wurzite compounds. This, together with exploration of novel quantum structures as well as of co-doping and co-alloying, may lead to fabrication of functional systems.

On the theoretical side, further work is necessary to evaluate quantitative corrections to the mean field theory brought about by thermodynamic fluctuations of magnetization. Effects of disorder associated with both random distribution of magnetic ions and fluctuations of carrier density near the metal-insulator transition are other open issues. In particular, unknown is the nature of evolution of static and dynamic magnetic phenomena on approaching the strongly localized regime. The above list of interesting problems is by no means exhausting. With no doubt we will soon witness many unforeseen developments in the field of carrier-mediated ferromagnetism in semiconductors.

ACKNOWLEDGMENTS

The work at Tohoku University was supported by the Japan Society for the Promotion of Science and by the Ministry of Education, Japan; the work in Poland by State Committee for Scientific Research, Grant No. 2-P03B-02417, and by Foundation for Polish Science.

APPENDIX A: EFFECTIVE-MASS HAMILTONIANS

The purpose of this Appendix is to provide the explicit form of the effective mass hamiltonian that, in addition to the standard kp and strain terms,³⁹ contains a contribution of the p-d exchange interaction in the molecular field approximation. The latter constitutes a generalization of the previous approaches^{40,66} by allowing for the arbitrary orientation of the magnetization M with respect to the crystal axes.

Zinc-blende semiconductors are considered first. We take explicitly into account four Γ_8 and two Γ_7 valence subbands, for which we chose the basis functions in the form:

$$u_1 = \frac{1}{\sqrt{2}}(X + iY) \uparrow, \quad (\text{A1})$$

$$u_2 = i\frac{1}{\sqrt{6}}[(X + iY) \downarrow - 2Z \uparrow], \quad (\text{A2})$$

$$u_3 = \frac{1}{\sqrt{6}}[(X - iY) \uparrow + 2Z \downarrow], \quad (\text{A3})$$

$$u_4 = i\frac{1}{\sqrt{2}}(X - iY) \downarrow, \quad (\text{A4})$$

$$u_5 = \frac{1}{\sqrt{3}}[(X + iY) \downarrow + Z \uparrow], \quad (\text{A5})$$

$$u_6 = i\frac{1}{\sqrt{3}}[-(X - iY) \uparrow + Z \downarrow], \quad (\text{A6})$$

where $X, Y,$ and Z denote Kohn-Luttinger amplitudes, which for the symmetry operations of the crystal point group transform as $p_x, p_y,$ and p_z wave functions of the hydrogen atom.

In the above basis the corresponding Luttinger-Kohn matrices assume the form:

1 kp matrix

$$H_{kp} = -\frac{\hbar^2}{2m_o} \begin{bmatrix} P+Q & L & M & 0 & iL/\sqrt{2} & -i\sqrt{2}M \\ L^* & P-Q & 0 & M & -i\sqrt{2}Q & i\sqrt{3/2}L \\ M^* & 0 & P-Q & -L & -i\sqrt{3/2}L^* & -i\sqrt{2}Q \\ 0 & M^* & -L^* & P+Q & -iM^* & -iL^*/\sqrt{2} \\ -iL^*/\sqrt{2} & i\sqrt{2}Q & i\sqrt{3/2}L & i\sqrt{2}M & P+\Delta & 0 \\ i\sqrt{2}M^* & -i\sqrt{3/2}L^* & i\sqrt{2}Q & iL/\sqrt{2} & 0 & P+\Delta \end{bmatrix}. \quad (\text{A7})$$

Here,

$$P = \gamma_1 k^2, \quad (\text{A8})$$

$$Q = \gamma_2(k_x^2 + k_y^2 - 2k_z^2), \quad (\text{A9})$$

$$L = -i2\sqrt{3}\gamma_3(k_x - ik_y)k_z, \quad (\text{A10})$$

$$M = \sqrt{3}[\gamma_2(k_x^2 - k_y^2) - i2\gamma_3k_xk_y], \quad (\text{A11})$$

$$\Delta = 2m_o\Delta_o/\hbar^2. \quad (\text{A12})$$

2 p - d exchange matrix

$$H_{pd} = B_G \begin{bmatrix} 3b_xw_z & i\sqrt{3}b_xw_- & 0 & 0 & \sqrt{6}b_xw_- & 0 \\ -i\sqrt{3}b_xw_+ & (2b_z - b_x)w_z & 2ib_zw_- & 0 & i\sqrt{2}(b_x + b_z)w_z & -\sqrt{2}b_zw_- \\ 0 & -2ib_zw_+ & -(2b_z - b_x)w_z & i\sqrt{3}b_xw_- & \sqrt{2}b_zw_+ & -i\sqrt{2}(b_x + b_z)w_z \\ 0 & 0 & -i\sqrt{3}b_xw_+ & -3b_xw_z & 0 & -\sqrt{6}b_xw_+ \\ \sqrt{6}b_xw_+ & -i\sqrt{2}(b_x + b_z)w_z & \sqrt{2}b_zw_- & 0 & -(2b_x - b_z)w_z & ib_zw_- \\ 0 & -\sqrt{2}b_zw_+ & i\sqrt{2}(b_x + b_z)w_z & -\sqrt{6}b_xw_- & -ib_zw_+ & (2b_x - b_z)w_z \end{bmatrix}. \quad (\text{A13})$$

Here,

$$B_G = \beta M/6g\mu_B, \quad (\text{A14})$$

$$w_z = M_z/M, \quad (\text{A15})$$

$$w_{\pm} = (M_x \pm iM_y)/M, \quad (\text{A16})$$

$$b_z = \beta_z/\beta, \quad (\text{A17})$$

$$b_x = \beta_x/\beta, \quad (\text{A18})$$

where in cubic materials $b_z = b_x = 1$.

3 Biaxial strain matrix

$$H_{bs} = b \begin{bmatrix} -Q_\epsilon & 0 & R_\epsilon & 0 & 0 & -i\sqrt{2}R_\epsilon \\ 0 & Q_\epsilon & 0 & R_\epsilon & i\sqrt{2}Q_\epsilon & 0 \\ R_\epsilon & 0 & Q_\epsilon & 0 & 0 & i\sqrt{2}Q_\epsilon \\ 0 & R_\epsilon & 0 & -Q_\epsilon & -i\sqrt{2}R_\epsilon & 0 \\ 0 & -i\sqrt{2}Q_\epsilon & 0 & i\sqrt{2}R_\epsilon & 0 & 0 \\ i\sqrt{2}R_\epsilon & 0 & -i\sqrt{2}Q_\epsilon & 0 & 0 & 0 \end{bmatrix}. \quad (\text{A19})$$

Here, b is the deformation potential and

$$Q_\epsilon = \epsilon_{zz} - (\epsilon_{xx} + \epsilon_{yy})/2, \quad (\text{A20})$$

$$R_\epsilon = \sqrt{3}(\epsilon_{xx} - \epsilon_{yy})/2. \quad (\text{A21})$$

Since we are interested in the effect of the biaxial strain in the (001) plane, only the terms involving the diagonal components ϵ_{ii} of the deformation tensor are included. For the same reason, we allow for the corresponding anisotropy of the exchange integrals $\beta_x = \beta_y \neq \beta_z$, though we expect that to a good accuracy $\beta_x = \beta_z$ in real systems. The latter is assumed in the main body of the paper.

In the presence of the magnetic field B the Luttinger-Kohn kp matrix is a sum of the Zeeman and Landau parts, $H_{kp} = H_Z + H_L$, where H_L is written below for $\mathbf{B} \parallel [001]$ and neglecting some terms proportional to $\gamma_2 - \gamma_3$.⁸⁶

$$H_Z = -g_o\mu_B B \begin{bmatrix} 3\kappa w_z/2 & i\sqrt{3}\kappa w_-/2 & 0 & \dots \\ -i\sqrt{3}\kappa w_+/2 & \kappa w_z/2 & i\kappa w_- & \dots \\ 0 & -i\kappa w_+ & -\kappa w_z/2 & \dots \\ 0 & 0 & -i\sqrt{3}\kappa w_+/2 & \dots \\ -\sqrt{6}(\kappa+1)w_+/4 & i\sqrt{2}(\kappa+1)w_z/2 & -\sqrt{2}(\kappa+1)w_-/4 & \dots \\ 0 & \sqrt{2}(\kappa+1)w_+/4 & -i\sqrt{2}(\kappa+1)w_z/2 & \dots \\ \dots & 0 & -\sqrt{6}(\kappa+1)w_-/4 & 0 \\ \dots & 0 & -i\sqrt{2}(\kappa+1)w_z/2 & \sqrt{2}(\kappa+1)w_-/4 \\ \dots & i\sqrt{3}\kappa w_-/2 & -\sqrt{2}(\kappa+1)w_+/4 & i\sqrt{2}(\kappa+1)w_z/2 \\ \dots & -3\kappa w_z/2 & 0 & \sqrt{6}(\kappa+1)w_+/4 \\ \dots & 0 & (\kappa+1/2)w_z & -i(\kappa+1/2)w_- \\ \dots & \sqrt{6}(\kappa+1)w_-/4 & i(\kappa+1/2)w_+ & -(\kappa+1/2)w_z \end{bmatrix}, \quad (\text{A22})$$

where g_o is the Landé factor of the free electron, and

$$w_z = B_z/B \quad (\text{A23})$$

$$w_\pm = B_x \pm iB_y. \quad (\text{A24})$$

For the Landau quantum number $n > 0$

$$H_L = -\frac{\hbar^2}{2m_o} \begin{bmatrix} h_h + s(\gamma_1 + \gamma_2)(2n-1) & b\sqrt{n} & c\sqrt{n(n+1)} & \dots \\ -b\sqrt{n}h_l + s(\gamma_1 - \gamma_2)(2n+1) & 0 & c\sqrt{(n+1)(n+2)} & \dots \\ c\sqrt{n(n+1)} & 0 & h_l + s(\gamma_1 - \gamma_2)(2n+3) & \dots \\ 0 & c\sqrt{(n+1)(n+2)} & b\sqrt{n+2} & \dots \\ ib\sqrt{n/2} & iq + i\sqrt{2}\gamma_2s(2n+1) & ib\sqrt{3(n+1)/2} & \dots \\ ic\sqrt{2(n+1)n} & ib\sqrt{3(n+1)/2} & iq + i\sqrt{2}\gamma_2s(2n+3) & \dots \\ \dots & 0 & -ic\sqrt{2n(n+1)} & \dots \\ \dots & -iq - i\sqrt{2}s\gamma_2(2n+1) & ib\sqrt{3(n+1)/2} & \dots \\ \dots & -b\sqrt{(n+2)} & ib\sqrt{3(n+1)/2} & -iq - i\sqrt{2}\gamma_2s(2n+3) \\ \dots & h_h + (\gamma_1 + \gamma_2)s(2n+5) & -ic\sqrt{2(n+1)(n+2)} & ib\sqrt{(n+2)/2} \\ \dots & ic\sqrt{2(n+2)(n+1)} & h_s + \gamma_1s(2n+1) & 0 \\ \dots & ib\sqrt{(n+2)/2} & 0 & h_s + \gamma_1s(2n+3) \end{bmatrix}. \quad (\text{A25})$$

Here,

$$s = eB/\hbar, \quad (\text{A26})$$

$$h_h = (\gamma_1 - 2\gamma_2)k_z^2, \quad (\text{A27})$$

$$h_l = (\gamma_1 + 2\gamma_2)k_z^2, \quad (\text{A28})$$

$$h_s = \gamma_1 k_z^2, \quad (\text{A29})$$

$$q = -2\sqrt{2}\gamma_2 k_z^2, \quad (\text{A30})$$

$$b = -i2\sqrt{6}s\gamma_3 k_z; \quad (\text{A31})$$

$$c = \sqrt{3}s(\gamma_2 + \gamma_3). \quad (\text{A32})$$

If $n = 0$, the wave function basis does not contain the u_1 term, so that

$$H_L = -\frac{\hbar^2}{2m_o} \begin{bmatrix} h_l + s(\gamma_1 - \gamma_2)(2n + 1) & 0 & \sqrt{(n+2)(n+1)} & \dots \\ 0 & h_l + s(\gamma_1 - \gamma_2)(2n + 3) & -b\sqrt{n+2} & \dots \\ c\sqrt{(n+2)(n+1)} & b\sqrt{n+2} & h_h + (\gamma_1 + \gamma_2)s(2n + 5) & \dots \\ iq + i\sqrt{2}\gamma_2 s(2n + 1) & ib\sqrt{3(n+1)/2} & ic\sqrt{2(n+2)(n+1)} & \dots \\ ib\sqrt{3(n+1)/2} & iq + i\sqrt{2}\gamma_2 s(2n + 3) & ib\sqrt{(n+2)/2} & \dots \\ \dots & -iq - i\sqrt{2}s\gamma_2(2n + 1) & ib\sqrt{3(n+1)/2} & \dots \\ \dots & ib\sqrt{3(n+1)/2} & -iq - i\sqrt{2}\gamma_2 s(2n + 3) & \dots \\ \dots & -ic\sqrt{2(n+2)(n+1)} & ib\sqrt{(n+2)/2} & \dots \\ \dots & h_s + \gamma_1 s(2n + 1) & 0 & \dots \\ \dots & 0 & h_s + \gamma_1 s(2n + 3) & \dots \end{bmatrix}. \quad (\text{A33})$$

If $n = -1$, the wave function basis does not contain the u_1 , u_2 , and u_5 terms, so that

$$H_L = -\frac{\hbar^2}{2m_o} \begin{bmatrix} h_l + s(\gamma_1 - \gamma_2)(2n + 3) & -b\sqrt{n+2} & -iq - i\sqrt{2}\gamma_2 s(2n + 3) \\ b\sqrt{n+2} & h_h + (\gamma_1 + \gamma_2)s(2n + 5) & ib\sqrt{(n+2)/2} \\ iq + i\sqrt{2}\gamma_2 s(2n + 3) & ib\sqrt{(n+2)/2} & h_s + \gamma_1 s(2n + 3) \end{bmatrix}. \quad (\text{A34})$$

If $n=-2$, the wave function basis contains only u_4 term, so that

$$H_L = -\frac{\hbar^2}{2m_o} [h_h + (\gamma_1 + \gamma_2)s]. \quad (\text{A35})$$

The solution of the eigenvalue and eigenfunction problem for the hamiltonian $H = H_{kp} + H_{pd} + H_{bs}$ or, in the magnetic field, $H = H_L + H_Z + H_{pd} + H_{bs}$ gives the hole energies ε_i and eigenvectors $a_i^{(j)}$ for the six relevant hole subbands.

4 Wurzite compounds

For wurzite compounds, we chose the basis in the form,

$$u_1 = -\frac{1}{\sqrt{2}}(X + iY) \uparrow, \quad (\text{A36})$$

$$u_2 = \frac{1}{\sqrt{2}}(X - iY) \uparrow, \quad (\text{A37})$$

$$u_3 = Z \uparrow, \quad (\text{A38})$$

$$u_4 = \frac{1}{\sqrt{2}}(X - iY) \downarrow, \quad (\text{A39})$$

$$u_5 = -\frac{1}{\sqrt{2}}(X + iY) \downarrow \quad (\text{A40})$$

$$u_6 = Z \downarrow, \quad (\text{A41})$$

In the above basis, the kp matrix reads

$$\frac{\hbar^2}{2m_o} \begin{bmatrix} F & -K^* & -H^* & 0 & 0 & 0 \\ -K & F - 2\Delta_2 & H & 0 & 0 & \sqrt{2}\Delta_3 \\ -H & H^* & L - \Delta_1 - \Delta_2 & 0 & \sqrt{2}\Delta_3 & 0 \\ 0 & 0 & 0 & F & -K & H \\ 0 & 0 & \sqrt{2}\Delta_3 & -K^* & F - 2\Delta_2 & -H^* \\ 0 & \sqrt{2}\Delta_3 & 0 & H^* & -H & L - \Delta_1 - \Delta_2 \end{bmatrix}. \quad (\text{A42})$$

Here,

$$L = A_1 k_z^2 + A_2 (k_x^2 + k_y^2), \quad (\text{A43})$$

$$T = A_3 k_z^2 + A_4 (k_x^2 + k_y^2), \quad (\text{A44})$$

$$F = L + T, \quad (\text{A45})$$

$$k_+ = k_x + ik_y, \quad (\text{A46})$$

$$K = A_5 k_+^2, \quad (\text{A47})$$

$$H = A_6 k_+ k_z, \quad (\text{A48})$$

where Δ_i and A_i are the valence band splittings and kp parameters, respectively.

p-d exchange matrix is given by

$$H_{pd} = 3B_G \begin{bmatrix} b_x w_z & 0 & 0 & 0 & b_x w_m & 0 \\ 0 & b_x w_z & 0 & b_x w_m & 0 & 0 \\ 0 & 0 & b_z w_z & 0 & 0 & b_z w_m \\ 0 & b_x w_p & 0 & -b_x w_z & 0 & 0 \\ b_x w_p & 0 & 0 & 0 & -b_x w_z & 0 \\ 0 & 0 & b_z w_p & 0 & 0 & -b_z w_z \end{bmatrix}. \quad (\text{A49})$$

APPENDIX B: NUMERICAL PROCEDURE

We aim at evaluating the Helmholtz free energy F_c at given hole concentration p as a function of the Mn magnetization M ,

$$F_c(p, M) = -k_B T \int d\varepsilon N(\varepsilon) \ln(1 + \exp[-(\varepsilon(M) - \varepsilon_F(p, M))/k_B T]) + p\varepsilon_F(p, M), \quad (\text{B1})$$

where the thermodynamic density-of-states $N(\varepsilon) = \partial p / \partial \varepsilon$. If $T < 200$ K then in the studied cases the hole liquid is degenerate, so that F_c assumes a simple form,

$$F_c(p, M) = \int_0^p dp' \varepsilon(M, p'). \quad (\text{B2})$$

Thus, in order to obtain $F_c(p, M)$ we have to integrate the dependence of the partition function or of the Fermi energy on the hole concentration for various M . The actual calculation proceeds in a standard way. First, the length of the wave vectors $k_i(\theta, \varphi)$ for each of six hole subbands is determined by solving the inverse eigenvalue problem for given values of ε , polar angle θ and azimuth angle φ in the \mathbf{k} -vector space. Then, the hole concentration is obtained by an integration of $\sum_i k_i^3(\theta, \varphi) / 24\pi^3$ over $\cos\theta$ and φ .

In order to calculate the contribution M_c of the hole magnetic moments to the total magnetization, the eigenvalue problem is solved directly making it possible to determine the Gibbs thermodynamic potential G_c ,

$$G_c = - \sum_{i, n, k_z} k_B T (eB / 2\pi\hbar) \ln(1 + \exp[-(\varepsilon_i(n, k_z, M) - \varepsilon_F) / k_B T]). \quad (\text{B3})$$

We calculate the absorption coefficient α for the two circular polarizations σ^\pm , taking into account k conserving electron transitions from the six valence band subbands, index i , to the two spin branches of the conduction band, index j , assuming that the hole liquid is strongly degenerate. In such a model,^{87,88}

$$\alpha^\pm = \frac{4\pi^2 e^2 P^2}{\hbar^2 c n_r \omega} \sum_{i, j} \int_{-1}^1 d \cos \theta \int_0^{2\pi} d\varphi \frac{k_{ij}(\omega) m_r^{(ij)}(\omega)}{8\pi^3 \hbar^2} |M_{ij}^\pm|^2. \quad (\text{B4})$$

The wave vectors $k_{ij}(\omega, \theta, \varphi)$ corresponding to twelve possible transitions are determined by the energy conservation and the position of the Fermi level. The joint density of states effective mass corresponding to these k_{ij} is given by

$$m_r^{(ij)} = (1/m_e - \frac{1}{\hbar^2 k_{ij}} \frac{\partial \varepsilon_i}{\partial k_{ij}})^{-1}. \quad (\text{B5})$$

The matrix elements $M_{ij}^\pm(\theta, \varphi)$ for the two light polarizations and involving electron transitions to the spin down and spin up conduction subbands are given by

$$M_{i1}^+ = a_i^{(4)}, \quad (\text{B6})$$

$$M_{i2}^+ = a_i^{(3)}/\sqrt{3} + ia_i^{(6)}\sqrt{2/3}, \quad (\text{B7})$$

$$M_{i1}^- = a_i^{(2)}/\sqrt{3} - ia_i^{(5)}\sqrt{2/3}, \quad (\text{B8})$$

$$M_{i2}^- = a_i^{(1)}, \quad (\text{B9})$$

where a_i^n is the n -th component of the eigenvector corresponding i -th valence subband at $k_{ij}(\theta, \varphi)$.

APPENDIX C: MATERIAL PARAMETERS

In Tables I and II we summarize band structure parameters of parent compounds employed for the evaluation of chemical trends in cubic and wurzite magnetic semiconductors.

TABLE I: Material parameters of selected cubic semiconductors and the values of the p-d exchange energy βN_o . Except for the parameters for which references are provided, the values of the lattice constant a_o , spin-orbit splitting Δ_o , and Luttinger parameters γ_i are taken from *Landolt-Börstein*.^{65,79,89,90}

	a_o (Å)	Δ_o (eV)	γ_1	γ_2	γ_3	βN_o (eV)
Si	5.43	0.044	4.285	0.339	1.446	-1.35 ^a
Ge	5.66	0.29	13.38	4.24	5.69	-1.20 ^a
AlP	5.47	0.1 ^a	3.47	0.06	1.15	-1.33 ^a
AlAs	5.66	0.275	3.25	0.64	1.21	-1.19 ^a
GaN	4.50 ^b	0.018 ^b	2.463 ^c	0.647 ^c	0.975 ^c	-2.37 ^a
GaP	5.45	0.080	4.05	0.49	1.25	-1.34 ^a
GaAs	5.65	0.34	6.85	2.1	2.9	-1.2 ^d
GaSb	6.09	0.76	13.3	4.4	5.7	-0.96 ^a
InP	5.87	0.108	5.15	0.94	1.62	-1.07 ^a
InAs	6.06	0.38	20.4	8.3	9.1	-0.98 ^a
ZnS	5.401	0.070	1.77 ^a	0.30 ^a	0.62 ^a	-1.5 ^e
ZnSe	5.67	0.43	2.95 ^f	0.6 ^f	1.11 ^g	-1.3 ^h
ZnTe	6.10	0.91	3.8	0.72	1.3	-1.1 ⁱ
CdTe	6.48	0.95	4.14	1.09	1.62 ^j	-0.88 ^j

^a the value determined from Eq. (19)

^b the value determined from the data for the wurzite structure (Table II)

^c K. Kim, W.L.R. Lambrecht, B. Segall, and M. van Schilfgaarde, Phys. Rev. B **56**, 7363 (1997); in this paper the Dresselhaus parameters L, M, N are denoted as A, B, C , respectively; see also, I. Stolpe, N. Puhmann, H.-U. Müller, O. Portugall, M. von Ortenberg, D. Schikora, D.J. As, B. Schöttker, and R. Lischka, Physica B **256-258**, 659 (1998)

^d the value from photoemission.²⁴

^e the value determined from Eq. (20)

^f see the main body of the text

^g H.W. Hölscher, A. Nöthe, and Ch. Uihlein, Phys. Rev. B **31**, 2379 (1985)

^h magnetorefectivity⁸⁰

ⁱ magnetorefectivity⁴³

^j magnetorefectivity⁷²

TABLE II: Material parameters of selected wurzite semiconductors. The values of the lattice parameter $a_o = (\sqrt{3}a^2c)^{1/3}$ and the splittings Δ_i of the valence band at the Γ point in II-VI compounds are taken from *Landolt-Börstein*.^{79,89} Theoretical studies provide the parameters Δ_i and A_i for GaN,⁹¹ InN,⁹² and A_i for ZnO, CdS, and CdSe.⁷⁵

Material	GaN	InN	ZnO	CdS	CdSe
a_o (Å)	4.503	4.974	4.567	5.845	6.078
Δ_1 (eV)	0.0036	0.017	0.04	0.030	0.039
Δ_2 (eV)	0.005	0.001	0.0	0.022	0.139
Δ_3 (eV)	0.0059	0.001	0.0	0.022	0.139
A_1	-6.4	-9.28	-2.41	-5.92	-10.2
A_2	-0.5	-0.6	-0.44	-0.70	-0.76
A_3	5.9	8.68	2.11	5.37	9.53
A_4	-2.55	-4.34	-1.06	-1.82	-3.2
A_5	-2.56	-4.32	-1.06	-1.82	-3.2
A_6	-3.06	-6.08	-1.51	-1.36	-2.31
βN_o (eV)	-2.37 ^a	-1.76 ^a	-2.48 ^b	-1.55 ^c	-1.27 ^d

^a Calculated from Eq. (19)

^b Calculated from Eq. (20)

^c interpretation of magneto-optical data²²

^d magnetoabsorption⁹³

REFERENCES

- [†] Electronic address: dietl@ifpan.edu.pl; URL: www.ifpan.edu.pl/SL-2/s123.html
- ¹ H. Ohno, H. Munekata, T. Penney, S. von Molnàr, and L.L. Chang, Phys. Rev. Lett. **68**, 2664 (1992).
 - ² H. Ohno, A. Shen, F. Matsukura, A. Oiwa, A. Endo, S. Katsumoto, and Y. Iye, Appl. Phys. Lett. **69** 363 (1996).
 - ³ A. Haury, A. Wasiela, A. Arnoult, J. Cibert, S. Tatarenko, T. Dietl, and Y. Merle d'Aubigné, Phys. Rev. Lett. **79**, 511 (1997).
 - ⁴ D.Ferrand, J.Cibert, C.Bourgognon, S.Tatarenko, A.Wasiela, G.Fishman, A.Bonanni, H.Sitter, S.Koleśnik, J.Jaroszyński, A.Barcz, and T.Dietl, J. Crystal Growth and Physica B, in press; e-print: xxx.lanl.gov/cond-matt/9910131.
 - ⁵ See, S. Koshihara, A. Oiwa, M. Hirasawa, S. Katsumoto, Y. Iye, C. Urano, H. Takagi, and H. Munekata, Phys. Rev. Lett. **78**, 4617 (1997).
 - ⁶ Y. Ohno, D.K. Young, B. Beschoten, F. Matskura, H. Ohno, and D.D. Awschalom, Nature **402**, 790 (1999).
 - ⁷ F. Matsukura, H. Ohno, A. Shen, and Y. Sugawara, Phys. Rev. B **57**, R2037 (1998).
 - ⁸ T. Dietl, H. Ohno, F. Matsukura, J. Cibert, and D. Ferrand, Science **287**, 1019 (2000).
 - ⁹ H. Ohno, Science **281**, 951 (1998); J. Magn. Magn. Mater. **200**, 110 (1999); J.K. Furdyna, P. Schiffer, Y. Sasaki, S.J. Potashnik, and X.Y. Liu, in: *Optical Properties of Semiconductor Nanostructures*, edited by M.L. Sadowski, M. Potemski, and M. Grynberg (Kluwer, Dordrecht, 2000) p. 211.
 - ¹⁰ J. Cibert, P. Kossacki, A. Haury, D. Ferrand, A. Wasiela, Y. Merle d'Aubigné, A. Arnoult, S. Tatarenko, and T. Dietl, in Proceedings of 24th International Conference on Physics of Semiconductors, Jerusalem, August 1998, edited by D. Gershoni (World Scientific, Singapore), p.51.
 - ¹¹ T. Story, Acta Phys. Polon. A **91**, 173 (1997).
 - ¹² R. Shioda, K. Ando, T. Hayashi, and M. Tanaka, Phys. Rev. B **58**, 1100 (1998).
 - ¹³ A. Balzarotti, N. Motta, A. Kisiel, M. Zimnal-Starnawska, M.T. Czyżyk, and M. Podgórný Phys. Rev. B **31**, 7526 (1985).
 - ¹⁴ A. Oiwa, S. Katsumoto, A. Endo, M. Hirasawa, Y. Iye, H. Ohno, F. Matsukura, A. Shen, Y. Sugawara, Solid State Commun. **103**, 209 (1997).
 - ¹⁵ A. Van Esch, L. Van Bockstal, J. De Boeck, G. Verbanck, A.S. van Steenbrgen, P.J. Wellmann, B. Grietens, R. Bogaerts, F. Herlach, and G. Borghs, Phys. Rev. B **56**, 13103 (1997).
 - ¹⁶ H. Shimizu, T. Hayashi, T. Nishinaga, M. Tanaka, Appl. Phys. Lett. **74**, 398 (1999).
 - ¹⁷ T. Omiya, F. Matsukura, T. Dietl, Y. Ohno, T. Sakon, M. Motokawa, and H. Ohno, Physica E, in press.
 - ¹⁸ W. Walukiewicz, Phys. Rev. B **37**, 4760 (1988).
 - ¹⁹ M. Linnarsson, E. Janzn, B. Monemar, M. Kleverman, and A. Thildevkvist, Phys. Rev. B **55**, 6938 (1997).
 - ²⁰ N.S. Averkiev, A.A. Gutkin, E.B. Osipov, and M.A. Reshchikov, Fiz. Tekh. Poluprovodn. **21**, 1847 (1987) [Sov. Phys. Semicond. **21**, 1119 (1987)].
 - ²¹ F.C. Zhang and T.M. Rice Phys. Rev. B **37**, 3759 (1988).
 - ²² C. Benoit à la Guillaume, D. Scalbert, and T. Dietl, Phys. Rev. B **46**, 9853 (1992).
 - ²³ A.K. Bhattacharjee and C. Benoit à la Guillaume, Solid State Commun. **113**, 17 (2000).
 - ²⁴ J. Okabayashi, A. Kimura, O. Rader, T. Mizokawa, A. Fujimori, T. Hayashi, and M. Tanaka, Phys. Rev. B **58**, R4211 (1998).
 - ²⁵ J. Okabayashi, A. Kimura, T. Mizokawa, A. Fujimori, T. Hayashi, and M. Tanaka, Phys. Rev. B **59**, R2486 (1999).
 - ²⁶ for a review on DMS, see, e.g., T. Dietl, in *Handbook on Semiconductors*, edited by T.S. Moss (North-Holland, Amsterdam, 1994) vol. 3b, p. 1251.
 - ²⁷ W.A. Harrison and G.K. Straub, Phys. Rev. B **36**, 2695 (1987).
 - ²⁸ H. Akai, Phys. Rev. Lett. **81**, 3002 (1998).
 - ²⁹ M.A. Paalanen and R.N. Bhatt, Physica B **169**, 153 (1991).
 - ³⁰ M. Sawicki, T. Dietl, J. Kossut, J. Igalson, T. Wojtowicz, and W. Plesiewicz, Phys. Rev. Lett. **56**, 508 (1986).
 - ³¹ P. Glód, T. Dietl, M. Sawicki, and I. Miotkowski, Physica B **194-196**, 995 (1994).
 - ³² T. Dietl, A. Haury, and Y. Merle d'Aubigné, Phys. Rev. B **55**, R3347 (1997).
 - ³³ T. Dietl, J. Cibert, D. Ferrand, and Y. Merle d'Aubigné, Mater. Sci. Engin. B **63**, 103 (1999), and references therein.
 - ³⁴ T. Jungwirth, W.A. Atkinson, B.H. Lee, and A.H. MacDonald, Phys. Rev. B **59**, 9818 (1999).
 - ³⁵ D. Belitz and T.R. Kirkpatrick, Rev. Mod. Phys. **57**, 287 (1994), and references therein.
 - ³⁶ J. Szczytko, K. Świątek, M. Palczewska, A. Twardowski, T. Hayashi, M. Tanaka, and K. Ando, Phys. Rev. B **60**, 8304 (1999) .
 - ³⁷ J. Szczytko, W. Mac, A. Twardowski, F. Matsukura, and H. Ohno, Phys. Rev. B **59**, 12935 (1999).
 - ³⁸ B. Beschoten, P.A. Crowell, I. Malajovich, D.D. Awschalom, F. Matskura, A. Shen, and H. Ohno, Phys. Rev. Lett. **83**, 3073 (1999).
 - ³⁹ G.L. Bir and G.E. Pikus, *Symmetry and Strain-Induced Effects in Semiconductors* (Wiley, New York, 1974).
 - ⁴⁰ J.A. Gaj, J. Ginter, and R.R. Gałazka, Phys. Status Solidi (b) **89**, 655 (1978).
 - ⁴¹ Y. Nishikawa, Y. Satoh, and J. Yoshino, in: *Extended Abstracts of the 2nd Symposium of Spin-Related Phenomena in Semiconductors*, Sendai, January, 1997, p. 122, unpublished.
 - ⁴² Y. Shapira, S. Foner, P. Becla, D.N. Domingues, M.J. Naughton, and J.S. Brooks, Phys. Rev. B **33**, 356 (1986).
 - ⁴³ A.Twardowski, P. Świdorski, M. von Ortenberg, and R. Pauthenet, Solid State Commun. **50**, 509 (1984).
 - ⁴⁴ D.Ferrand, J.Cibert, C.Bourgognon, S.Tatarenko, A.Wasiela, G.Fishman, T. Andrearczyk, S.Koleśnik, J.Jaroszyński, T.Dietl, B. Barbara, and D. Dufeu, unpublished; J. Appl. Phys. **87**, 6451 (2000).
 - ⁴⁵ P.A. Wolff, R.N. Bhatt, and A.C. Durst, J. Appl. Phys. **79**, 5196 (1996).
 - ⁴⁶ R.N. Bhatt and Xin Wan, Intern. J. Modern Phys. C **10**, 1459 (1999).
 - ⁴⁷ C. Zener, Phys. Rev. **81**, 440 (1950); *ibid.* **83** 299 (1950); a similar model for the nuclear ferromagnetism was developed by H. Fröhlich and F.R.N. Nabarro, Proc. Roy.

- Soc. (London) A **175**, 382 (1940); see also, e.g., P. Leroux-Hugon, in: *New Developments in Semiconductors*, edited by P.R. Wallace, R. Harris, and M.J. Zuckermann (Noordhoff, Leyden, 1973) p. 63; M.A. Krivoglaz, Usp. Fiz. Nauk **111** (1973) 617 [Sov. Phys. Usp. **16**, 856(1974)]; E.A. Pashitskii and S.M. Ryabchenko, Fiz. Tver. Tela **21**, 545 (1979) [Sov. Phys. Solid State **21**, 322 (1979)].
- ⁴⁸ J. Blinowski, P. Kacman, and J.A. Majewski, in: *High Magnetic Fields in Semiconductor Physics II*, eds. G. Landwehr, W. Ossau (World Scientific, Singapore 1997), p. 861.
- ⁴⁹ R. Abolfath, J. Brum, and A.H. MacDonald, unpublished.
- ⁵⁰ W. Szymańska and T. Dietl, J. Phys. Chem. Solids **39**, 1025 (1978).
- ⁵¹ C. Kittel, *Solid State Physics*, vol. 22, edited by F. Seitz, D. Turnbull, and H. Ehrenreich (Academic Press, New York, 1968), p. 1.
- ⁵² U. Larsen, Phys. Lett. **85A**, 471 (1981).
- ⁵³ P. Kossacki, D. Ferrand, A. Arnoult, J. Cibert, S. Tatarenko, A. Wasiela, Y. Merle d'Aubigné, K. Świątek, M. Sawicki, J. Wróbel, W. Bardyszewski, and T. Dietl, Physica E **6**, 709 (2000).
- ⁵⁴ M.E. Fisher, S.-k. Ma, and B.G. Nickel, Phys. Rev. Lett. **29**, 917 (1972).
- ⁵⁵ See, J.M. Yeomans, *Statistical Mechanics of Phase Transitions*, (Oxford University Press, Oxford, 1993), p. 57.
- ⁵⁶ K. Nishizawa and O. Sakai, in: *Extended Abstracts, 4th Symposium on the Spin-Related Phenomena in Semiconductors*, Sendai, December, 1998, p. 140, unpublished.
- ⁵⁷ M.A. Boselli, A. Ghazali, and I.C. da Cunha Lima, e-print: xxx.lanl.gov/cond-matt/0002254.
- ⁵⁸ J. König, H.-H. Lin, and A.H. MacDonald, Phys. Rev. Lett. **84**, 5628 (2000).
- ⁵⁹ M. Shirai, T. Ogawa, I. Kitagawa, and N. Suzuki J. Magn. Mater. **177-181**, 1383 (1998).
- ⁶⁰ R. Kato and H. Katayama-Yoshida, in: *Extended Abstracts of the 5th Symposium of Spin-Related Phenomena in Semiconductors*, Sendai, December, 1999, p. 233, unpublished.
- ⁶¹ P.T.J. Eggenkamp, H.J.M. Swagten, T. Story, V.I. Litvinov, C.H.W. Swüste, and W.J.M. de Jonge, Phys. Rev. B **51**, 15 250 (1995).
- ⁶² H. Ohno, F. Matsukura, T. Omiya, and N. Akiba, J. Appl. Phys. **85**, 4277 (1999).
- ⁶³ H. Ohno, F. Matsukura, A. Shen, Y. Sugawara, A. Oiwa, A. Endo, S. Katsumoto, and Y. Iye, in: *Proc. 23rd International Conference on the Physics of Semiconductors*, Berlin 1996, edited by M. Scheffler and R. Zimmermann (World Scientific, Singapore, 1996) p. 405.
- ⁶⁴ A. Hubert and R. Schafer, *Magnetic Domains* (Springer, Berlin, 1998).
- ⁶⁵ D. Bimberg et al., *Landolt-Börstein*, New-Series, vol. III/17a, edited by O. Madelung, M. Schulz, and W. Weiss (Springer, Berlin, 1982).
- ⁶⁶ see, *Diluted Magnetic Semiconductors*, edited by J.K. Furdyna and J. Kossut, Semiconductors and Semimetals, vol. 25 (Academic Press, Boston, 1988).
- ⁶⁷ J. Szczytko, W. Mac, A. Stachow, A. Twardowski, P. Becla, and J. Tworzydło, Solid State Commun. **99**, 927 (1996).
- ⁶⁸ K. Ando, T. Hayashi, M. Tanaka, and A. Twardowski, J. Appl. Phys. **83**, 6548 (1998).
- ⁶⁹ J. Cibert, P. Kossacki, A. Hauray, A. Wasiela, Y. Merle d'Aubigné, T. Dietl, A. Arnoult, and S. Tatarenko, *Proc. Intl. Conf. II-VI Compounds*, Grenoble 1997, J. Crystal Growth **184/185**, 898 (1998).
- ⁷⁰ H.C. Casey Jr. and F.F. Stern, J. Appl. Phys. **47**, (1976) 631.
- ⁷¹ H.C. Casey Jr., D.D. Sell, and K.W. Wecht, J. Appl. Phys. **46**, 250 (1975).
- ⁷² J.A. Gaj, R. Planel, and G. Fishman, Solid State Commun. **29**, 435 (1979).
- ⁷³ S. Lankes, M. Meier, T. Reisinger, and W. Gebhard, J. Appl. Phys. **80**, 4049 (1996).
- ⁷⁴ H.W. Hölscher, A. Nöthe, and Ch. Uihlein, Phys. Rev. B **31**, 2379 (1985).
- ⁷⁵ The parameters γ_i zinc-blende structure ZnS and ZnSe and A_i wurzite ZnO, CdS, and CdSe were obtained by fitting the corresponding kp model to the results of band structure computations given in D. Vogel, P. Krüger, and J. Pollmann, Phys. Rev. B **54**, 5495 (1996).
- ⁷⁶ H. Venghaus, Phys. Rev. B **19**, 3071 (1979).
- ⁷⁷ T. Mizokawa, J. Okabayashi, T. Nambu, and A. Fujimori, in: *Extended Abstracts of the 5th Symposium of Spin-Related Phenomena in Semiconductors*, Sendai, December 1999, unpublished.
- ⁷⁸ S. Katsumoto, A. Oiwa, Y. Iye, H. Ohno, F. Matsukura, A. Shen, and Y. Sugawara, phys. status solidi (b) **205**, 115 (1998).
- ⁷⁹ R. Blachnik et al., *Landolt-Börstein*, New Series, vol. 41B, edited by U. Rössler (Springer-Verlag, Berlin, 1999).
- ⁸⁰ A. Twardowski, M. von Ortenberg, M. Demianiuk, and R. Pauthenet, Solid State Commun. **51**, 849 (1984).
- ⁸¹ T. Wojtowicz, T. Dietl, M. Sawicki, W. Plesiewicz, and J. Jaroszyński, Phys. Rev. Lett. **56**, 2419 (1986).
- ⁸² M. Chmielowski, T. Dietl, P. Sobkowicz, and F. Koch, in: *Proc. 18th Int. Conf. Physics of Semiconductors*, Stockholm 1986, ed. O. Engström (World Scientific, Singapore, 1987) p. 1787.
- ⁸³ H. Hirakawa, S. Katsumoto, Y. Hashimoto, and Y. Iye, in: *Extended Abstracts of the 5th Symposium of Spin-Related Phenomena in Semiconductors*, Sendai, December, 1999, p. 174, unpublished.
- ⁸⁴ Y. Nagai, K. Nagasaka, H. Nojiri, M. Motokawa, F. Matsukura, and H. Ohno, in: *Extended Abstracts of the 5th Symposium of Spin-Related Phenomena in Semiconductors*, Sendai, December, 1999, p. 176, unpublished.
- ⁸⁵ T. Kamatani and H. Akai, in: *Extended Abstracts, 5th Symposium on the Spin-Related Phenomena in Semiconductors*, Sendai, December, 1999, p. 18, unpublished.
- ⁸⁶ R.R. Goodman, Phys. Rev. **122**, 397 (1961).
- ⁸⁷ E.O. Kane, J. Phys. Chem. Solids **1**, 249 (1957).
- ⁸⁸ We thank James J. Niggemann for his assistance in the derivation of momentum matrix elements.
- ⁸⁹ I. Broser et al., *Landolt-Börstein*, New Series, vol. 17b, edited by O. Madelung, M. Schulz, and W. Weiss, (Springer-Verlag, Berlin, 1982).
- ⁹⁰ O. Madelung, W. von der Osten, U. Rössler, *Landolt-Börstein*, New Series, vol. 22a, edited by O. Madelung (Springer-Verlag, Berlin, 1987).
- ⁹¹ K. Kim, W.L.R. Lambrecht, B. Segall, and M. van Schilf-

gaarde, Phys. Rev. B **56**, 7363 (1997); similar values of the kp parameters A_i M. Suzuki, T. Uenoyama, and A. Yanase, Phys. Rev. B **53**, 8132 (1995); J.A. Majewski, M. Städele, and P. Vogl, in: III-V Nitrides, edited by T. Moustakas, B. Monemar, I. Akasaki, and F. Ponce, *Materials Research Society Symposium Proceedings No 449*, (MRS, Pittsburg, 1997); for the review see, *Properties, Processing and Application of GaN and Related Semiconductors*, edited by J.H. Edgar, S. Strite, I. Akasaki, H. Amano, and C. Wetzel, An INSPEC Publication, pp. 153-207.

⁹² Y.C. Yeo, T.C. Chong, and M.F. Li, J. Appl. Phys. **83**, 1429 (1998).

⁹³ M. Arciszewska and M. Nawrocki, J. Phys. Chem. Solids **47**, 309 (1986).